

The Power of Density Functional Theory for Materials Physics and Chemistry

Date 11.07.18

Keith Refson



ROYAL
HOLLOWAY
UNIVERSITY
OF LONDON

About Me

Department
Of Physics

- PhD – Edinburgh Physics
- Postdoc IBM Kingston NY
- Research Associate Oxford
- Computational Scientist at STFC (Scientific Computing)
- Joint appointment Royal Holloway and ISIS



402

Acta Cryst. (1986). B42, 402–410

The Structure and Orientational Disorder in Solid *n*-Butane by Neutron Powder Diffraction

BY K. REFSON AND G. S. PAWLEY

Department of Physics, University of Edinburgh, Mayfield Road, Edinburgh EH9 3JZ, Scotland

(Received 12 August 1985; accepted 24 March 1986)

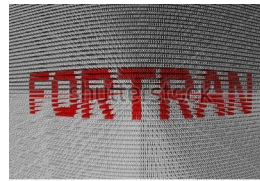
Abstract

The structure of deuterated *n*-butane (C_4H_{10}), $M_r = 68$, has been determined in its three crystalline forms by neutron powder diffraction with $\lambda = 2.980 \text{ \AA}$. All three have two molecules in the unit cell and space group $P2_1/c$. The stable phase III at 5 K has unit cell

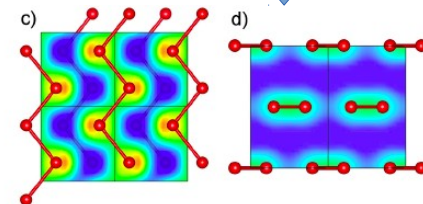
1979) on the other hand show a high degree of disorder and have no particular rotation axis. *n*-Butane (C_4H_{10}) is intermediate between these extremes as it has a low symmetry but is only four units long. It is of particular interest to compare the structure with 1,2-dichloroethane which has the same molecular



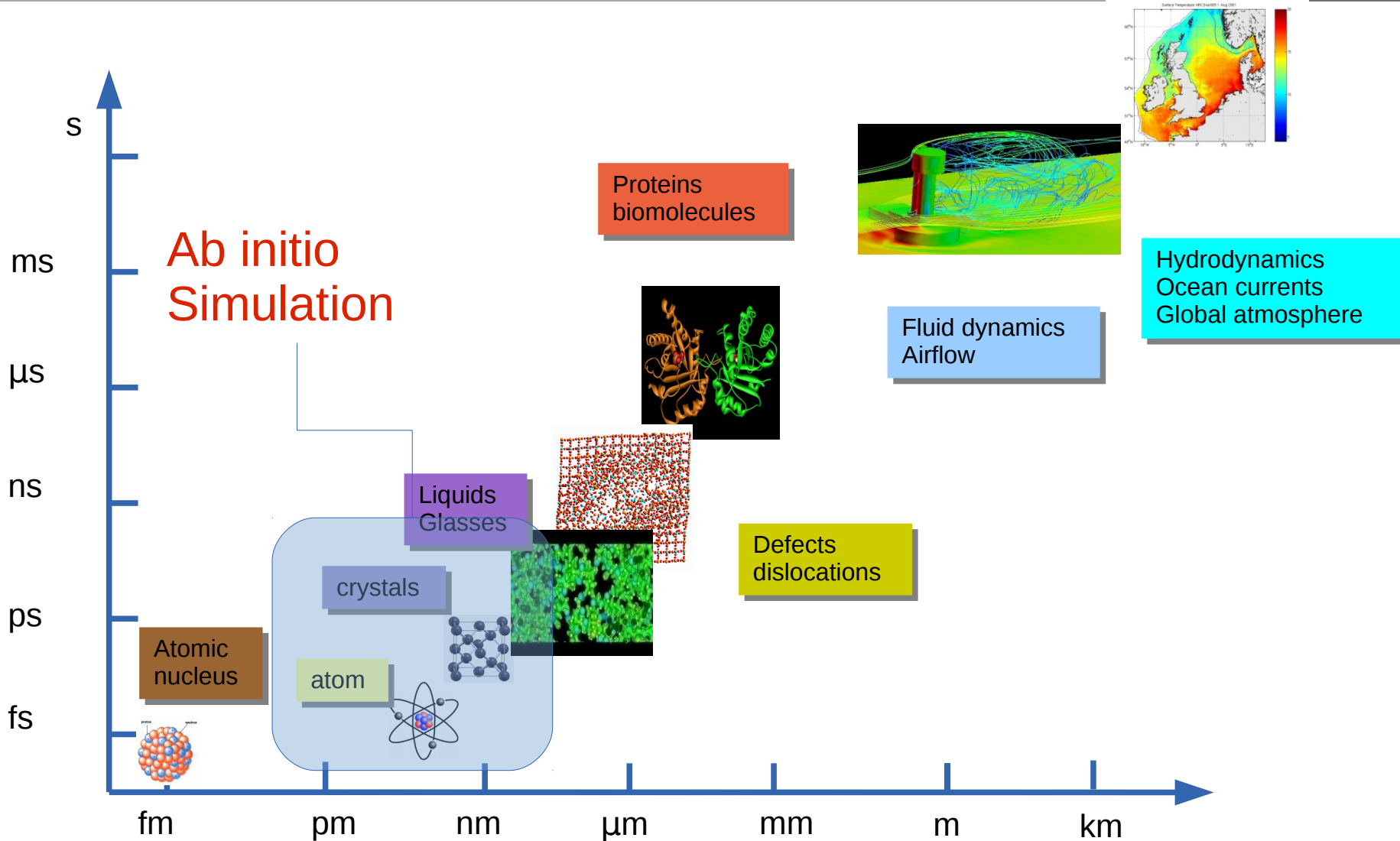
The CASTEP Project

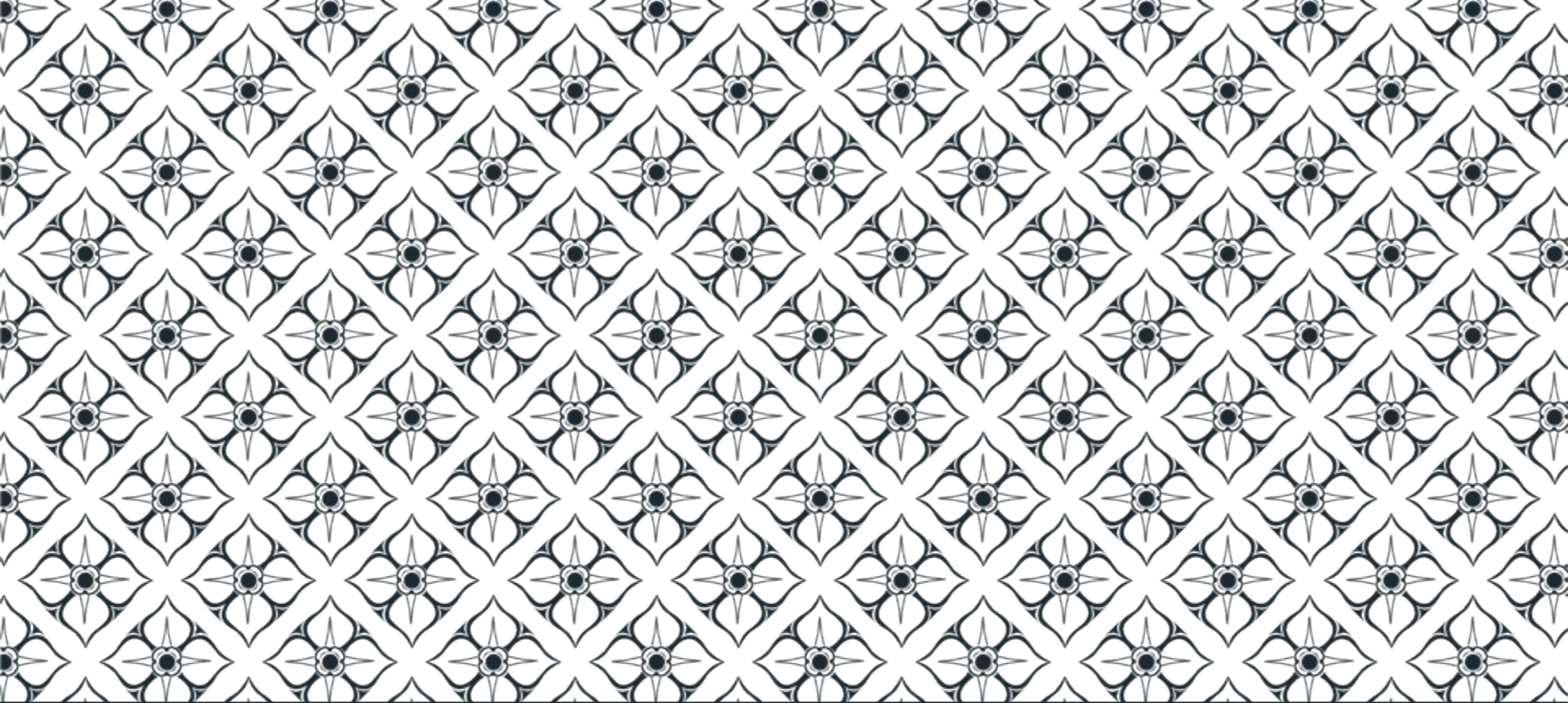


$$\left\{ \frac{1}{2} \nabla^2 + V_{\text{ext}}(\vec{r}) + V_H(\vec{r}) + V_{\text{xc}}([n(\vec{r})]) \right\} \phi_i(\vec{r}) = \epsilon_i \phi_i(\vec{r})$$



Simulation scales

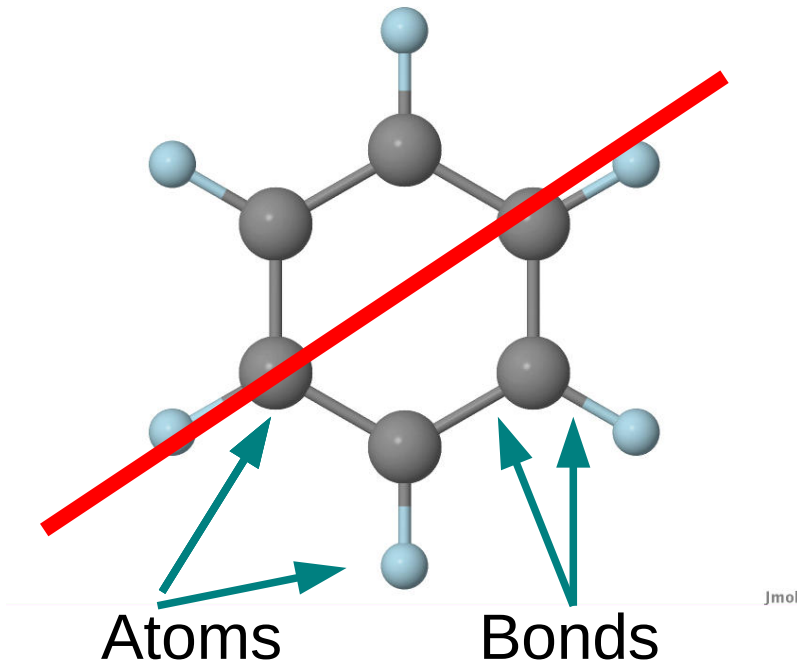




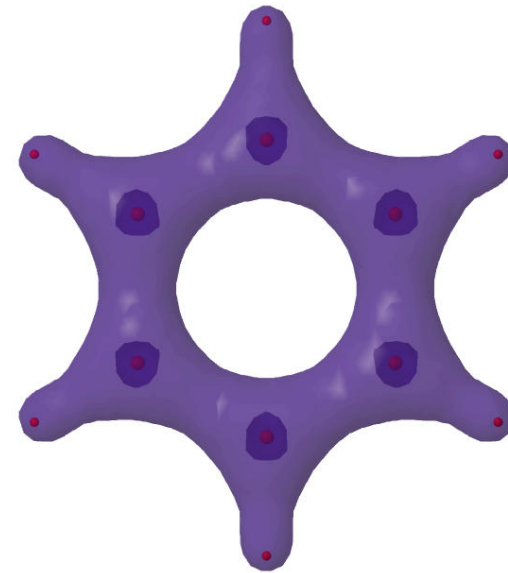
Quantum Mechanics and Density Functional Theory



The quantum Toolbox



$$F = m a$$



Nuclei

Electrons

$$\frac{-\hbar^2}{2m_e} \Psi + \hat{V} \Psi = E \Psi$$

The Theory of Everything

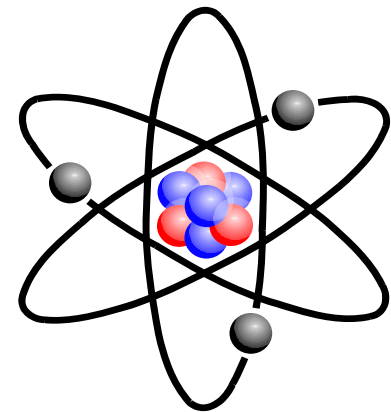
“The underlying physical laws necessary for the mathematical theory of a large part of physics and the whole of chemistry are thus completely known, and the difficulty is only that the application of these laws leads to equations much too complicated to be soluble.”

P.A.M. Dirac, Proceedings of the Royal Society **A123**, 714 (1929)

Why?

Each electron interacts with the nucleus
Every electron also interacts with every **other** electron.

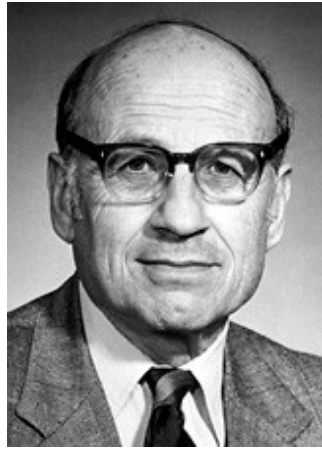
In Lithium ($Z=3$) there are **3 e-e interactions** to consider.
In Boron ($Z=5$) there are **10 e-e interactions** to consider.
In Iron ($Z=26$) there are **325 e-e interactions** to consider.
In Uranium ($Z=92$) there are **4186 e-e interactions** to consider.



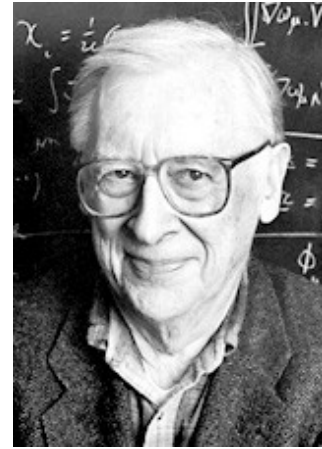
.. and that's just isolated atoms. We need to model crystals and molecules containing hundreds of atoms.

**QM of multi-electron atoms still too complex to solve on
Powerful supercomputers in 2016.**

Approximate quantum mechanics



Walter Kohn 1923-2016



John Pople 1925-2004

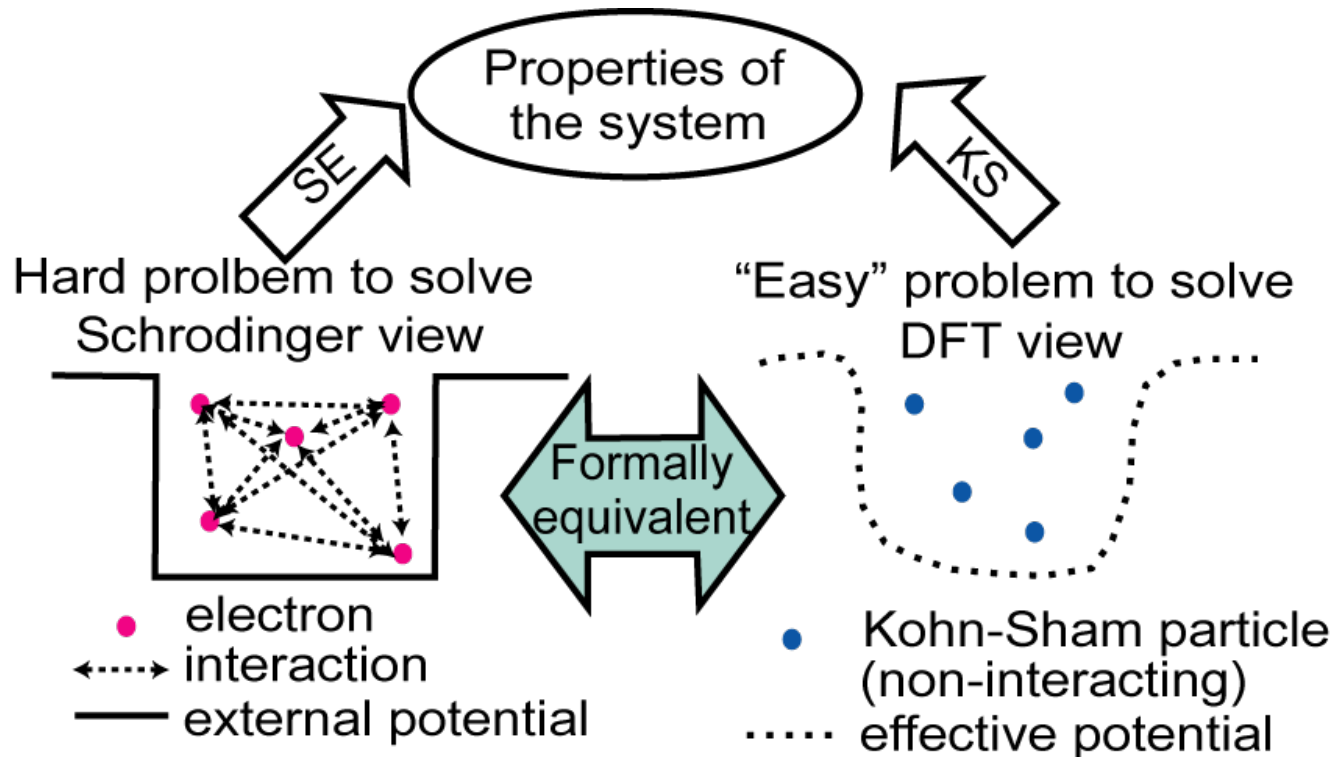
The Nobel Prize in Chemistry 1998 was divided equally between Walter Kohn "for his development of the **density-functional theory**" and John A. Pople "for his development of computational methods in **quantum chemistry**".

Key developments dating back to 1960s and 70s were approximate quantum theories which were nevertheless "good enough".

Density Functional Theory- Local Density Approximation

Hartree-Fock approximation, MP2, CI, CCSD(S,T)

Density Functional Theory

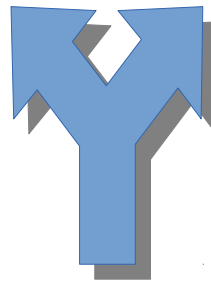
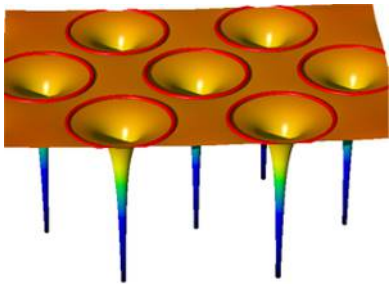


Approximate e-e interaction with

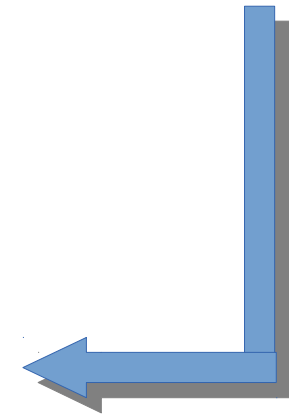
- local density approximation (LDA)
- generalized gradient approximation (GGA)
- Hybrids, DMFT, GW, ...

Kohn-Sham equations

$$\left\{ \frac{1}{2} \nabla^2 + V_{\text{ext}}(\vec{r}) + V_H(\vec{r}) + V_{\text{xc}}([n(\vec{r})]) \right\} \phi_i(\vec{r}) = \epsilon_i \phi_i(\vec{r})$$



$$n(\vec{r}) = \sum_i^{\text{occ}} |\phi_i(\vec{r})|^2$$



LDA and GGAs

LDA

$$V_{xc}[n] \approx V_{xc}(n(\vec{r}))$$

$$V_{xc} \equiv \frac{\delta E_{xc}[n]}{\delta n(\vec{r})}$$

Parameterized from uniform electron gas

- Cohesive energies ~ 1eV too large
- lattice parameters and bond lengths -1-2%
- Band gaps too small
- Hund's rule for open shells not always obeyed
- Van der Waals forces not included

GGAs

$$V_{xc}[n] \approx V_{xc}(n(\vec{r}), \nabla n(\vec{r}))$$

e.g. PBE, PW91, BLYP, ...

Parameterized from non-uniform electron gas and atoms

- Cohesive energies ~ 100 meV
- lattice parameters and bond lengths -1-2%
- Band gaps too small
- Hund's rule for open shells not always obeyed
- Van der Waals forces not included

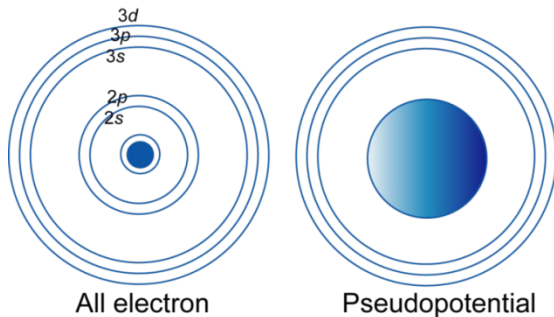
Plane-waves and pseudopotentials

Plane-wave basis set

$$\Psi_{n,\mathbf{k}}(\mathbf{r}) = u_{n,\mathbf{k}}(\mathbf{r})e^{i\mathbf{k}\mathbf{r}},$$
$$u_{n,\mathbf{k}}(\mathbf{r}) = \frac{1}{\Omega^{1/2}} \sum_{\mathbf{G}} C_{\mathbf{G}n\mathbf{k}} e^{i\mathbf{G}\mathbf{r}}$$

- Well-adapted for crystalline and solid/liquid modelling
- Systematic control of basis set convergence

Pseudopotential for ionic interactions

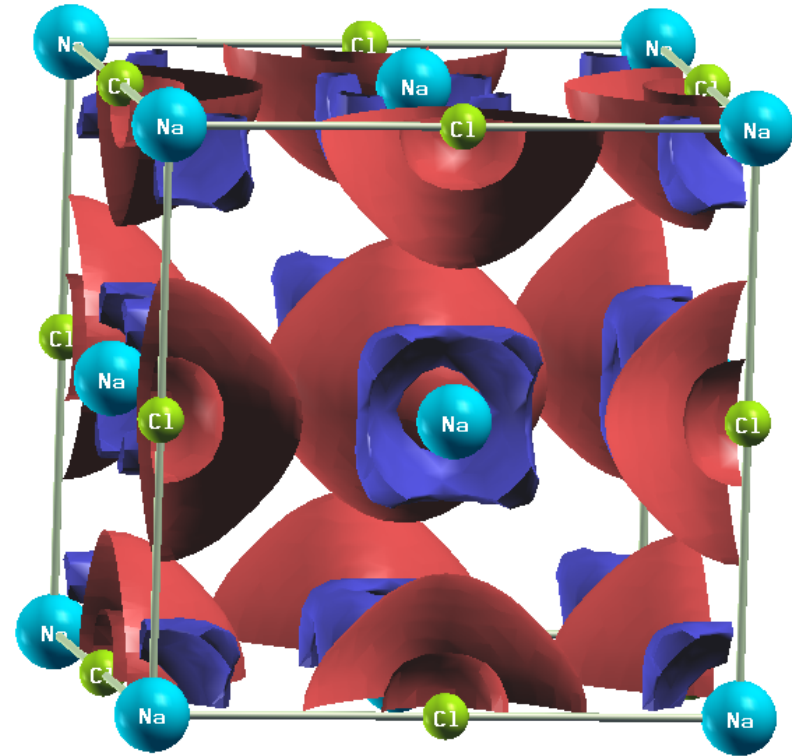


- “All electron” method but frozen core.
- Retain chemically relevant valence electrons
- Good scaling/large systems

Ionic bonding in NaCl

Charge transfer from Na to Cl

Unlike Si, no build up of charge between atoms



Covalent bonding in silicon

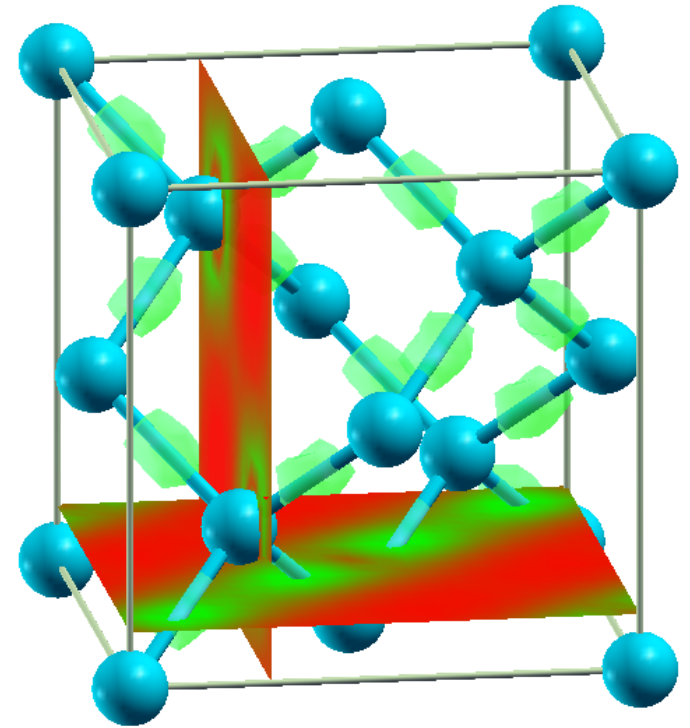
Covalent bonding arises from build up of -ve charge between +ve nuclei.

Chemical bond is **emergent property** of electron-ion system

Not merely qualitative description – can compute bond and cohesive energy.

($E_{\text{coh}} = 5.45 \text{ eV}$; expt 4.62 eV)

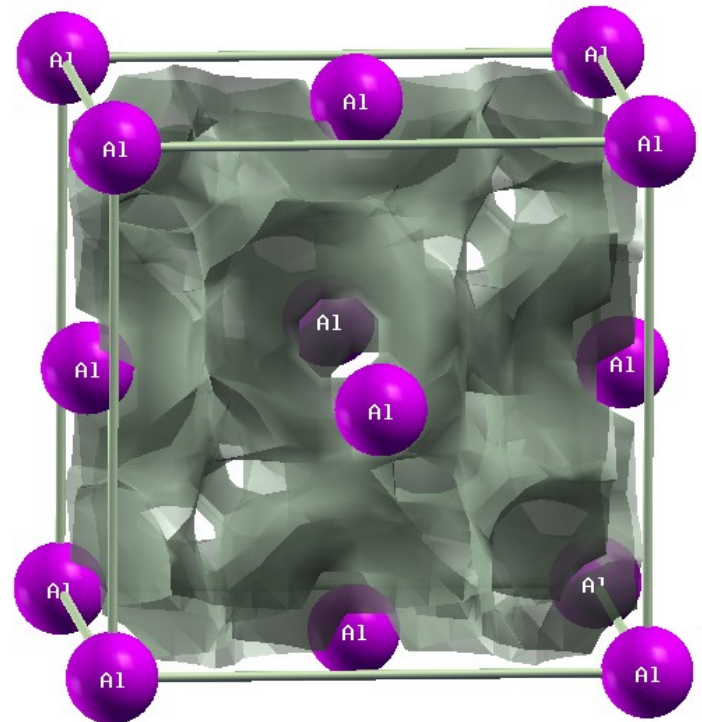
Lattice Parameter $a_0 = 0.549 \text{ nm}$ (0.5431 nm)



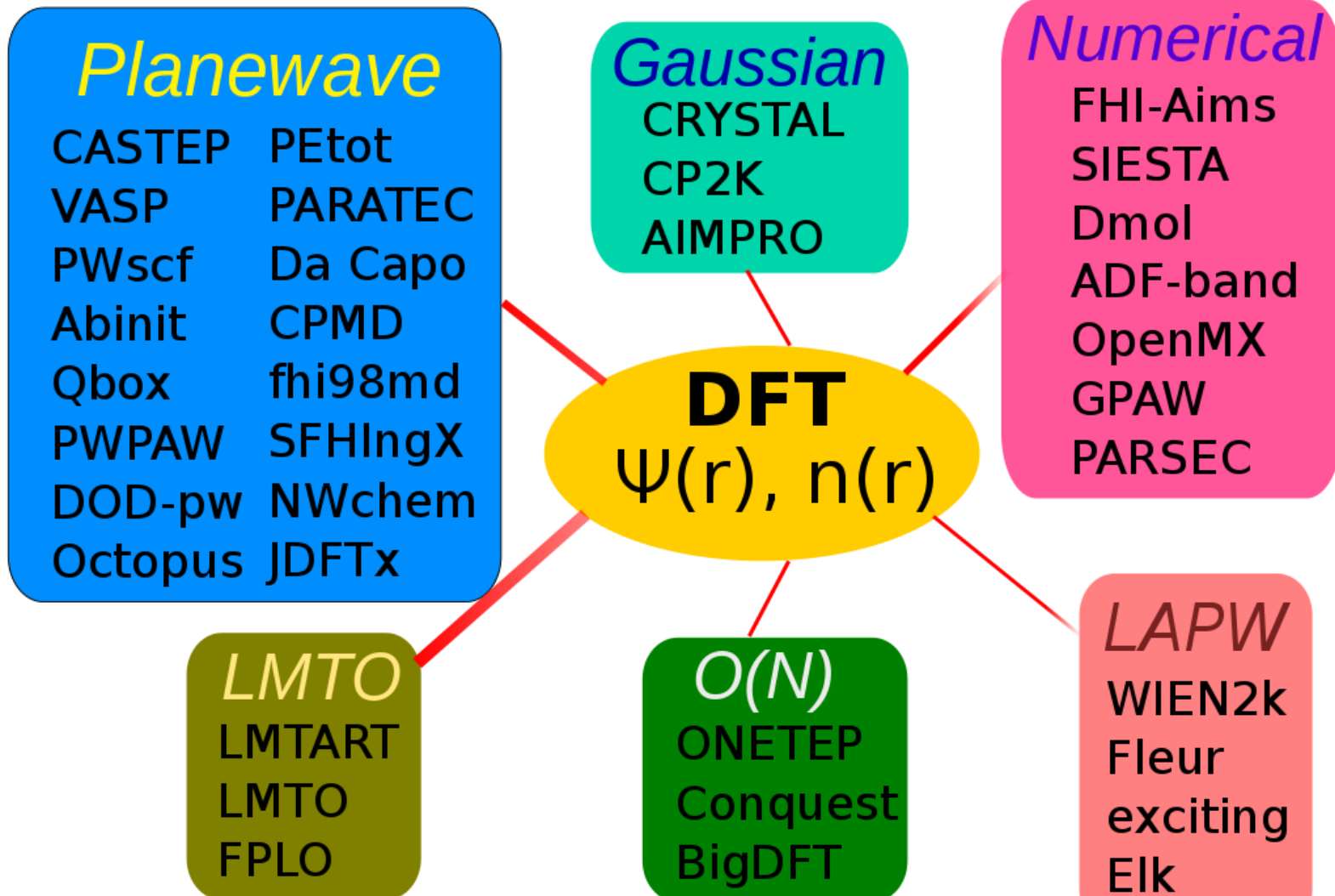
Metallic bonding in aluminium

Valence electrons are spread out – metallic state.

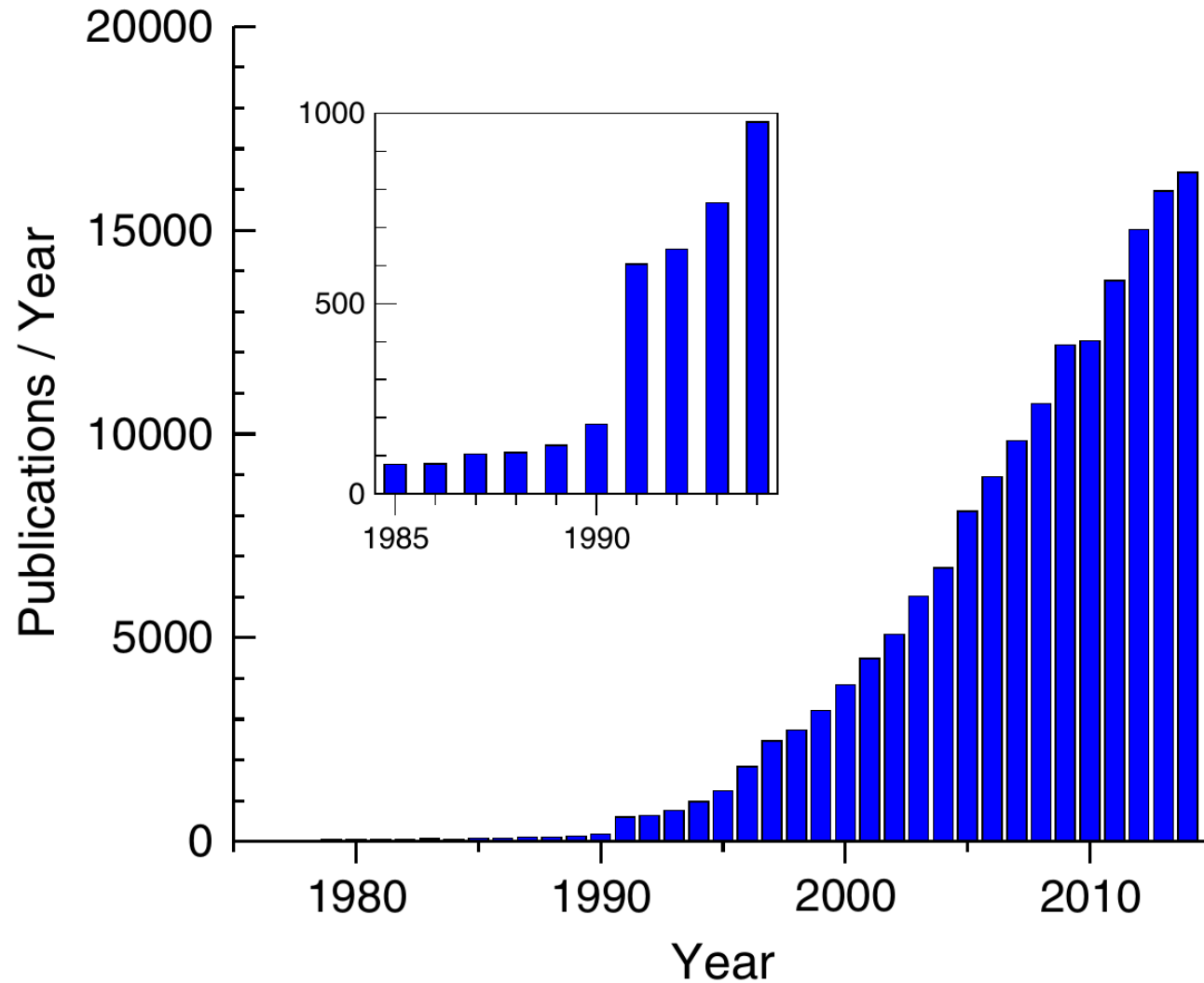
Calculation shows no **band gap**; correctly predicts Al is **metallic**.

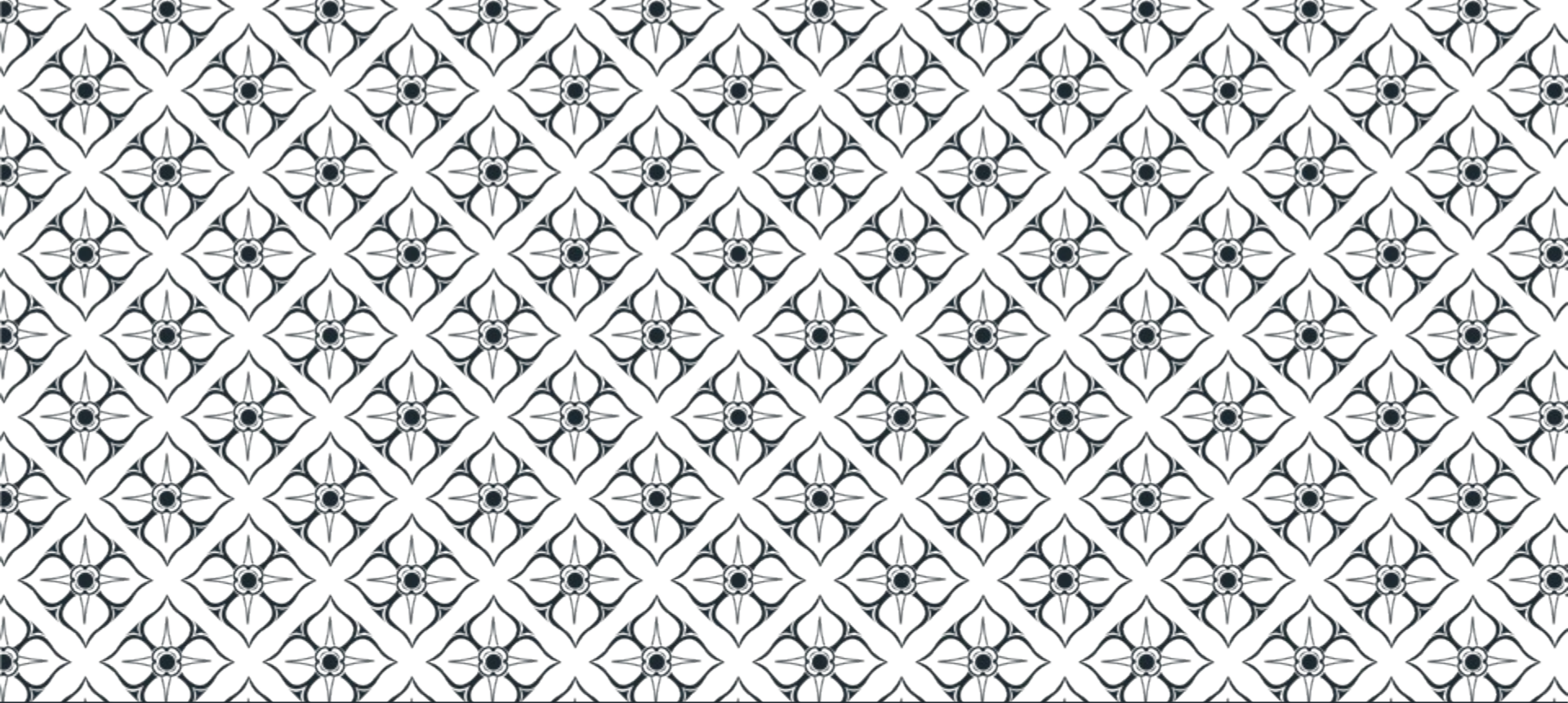


DFT Simulation Codes



Popularity of DFT

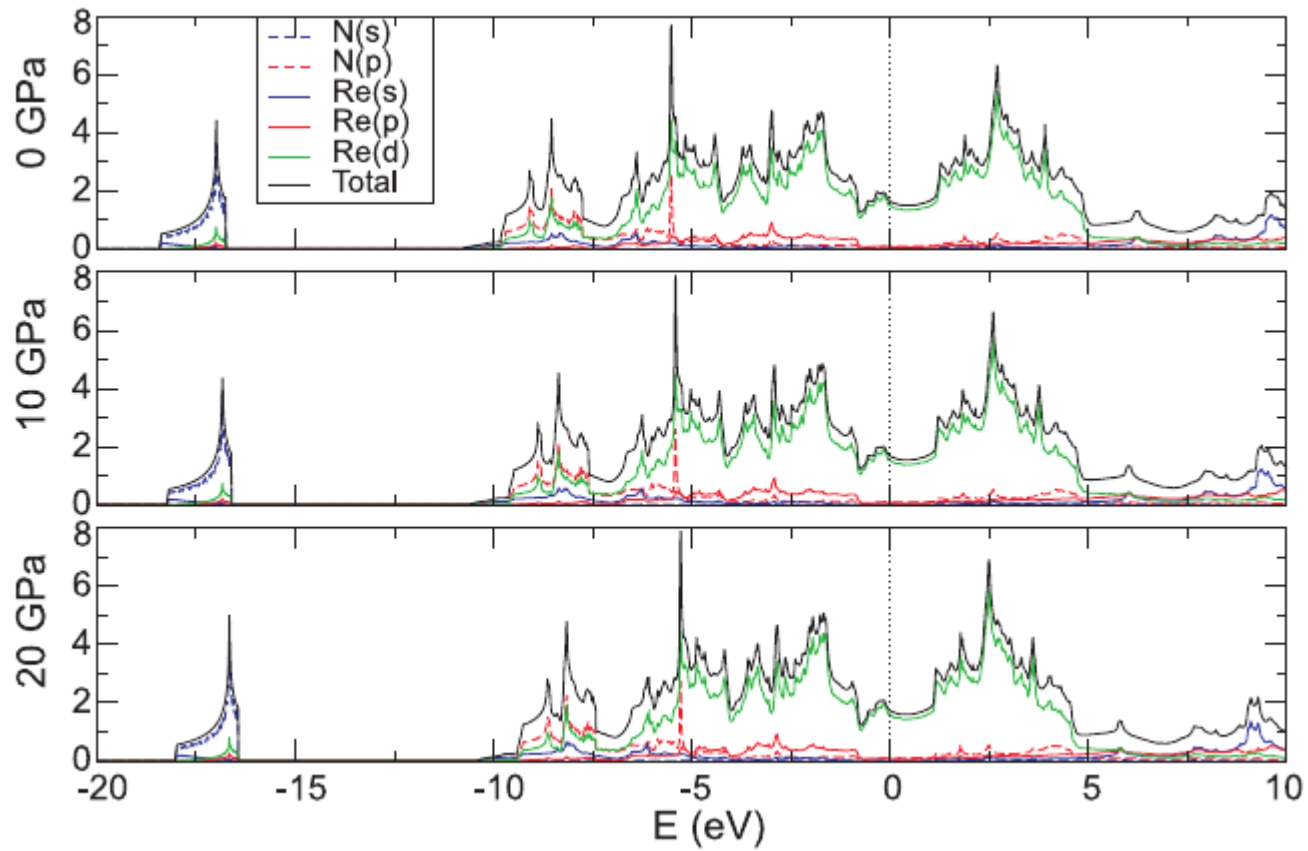




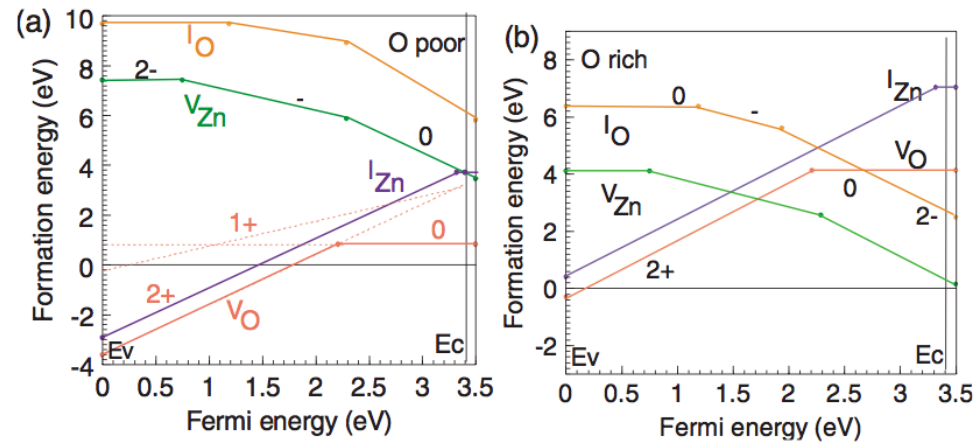
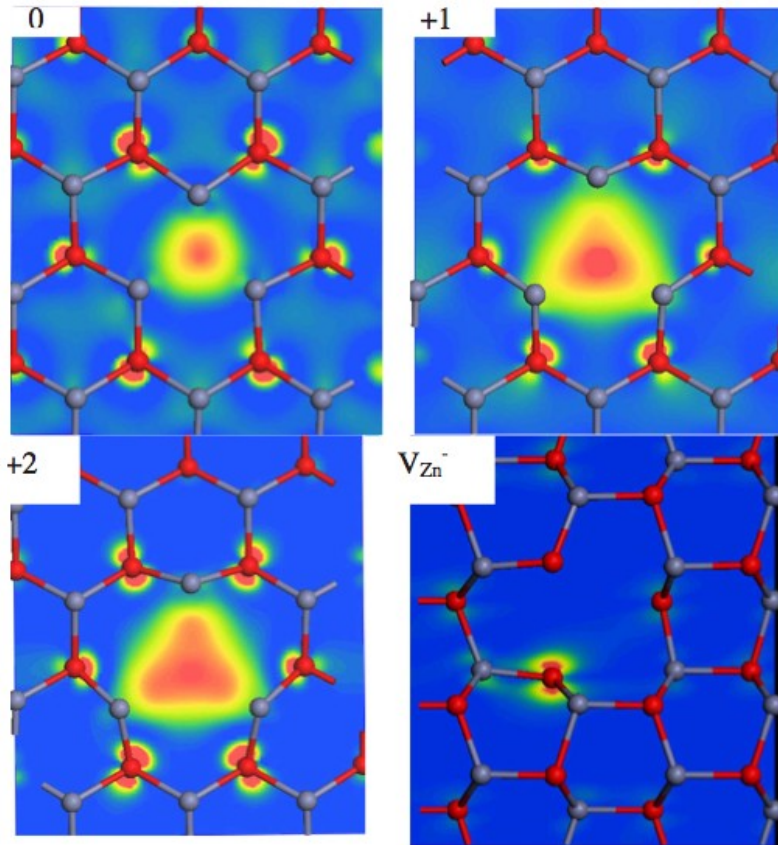
Electronic Structure



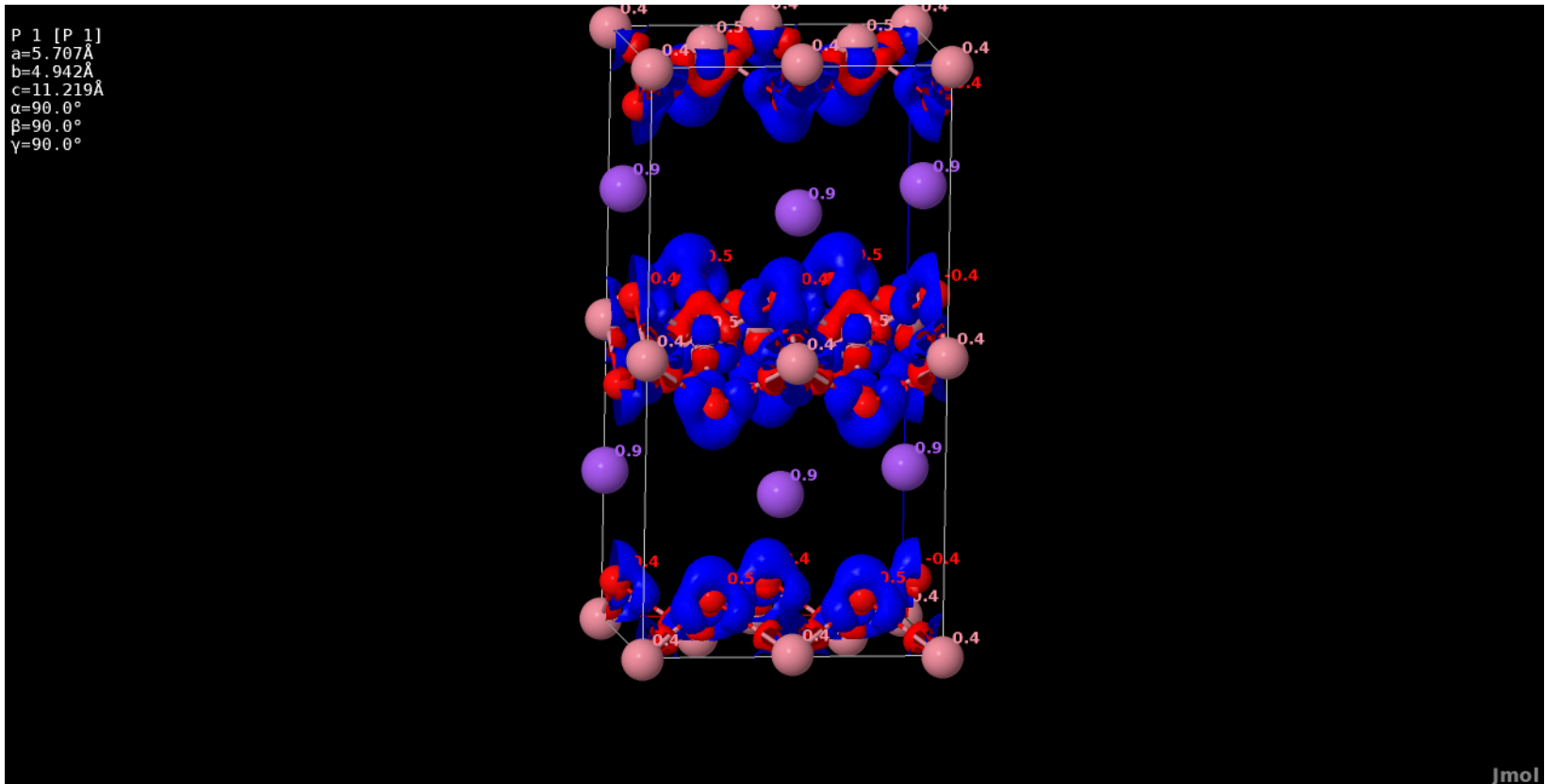
Densities of States

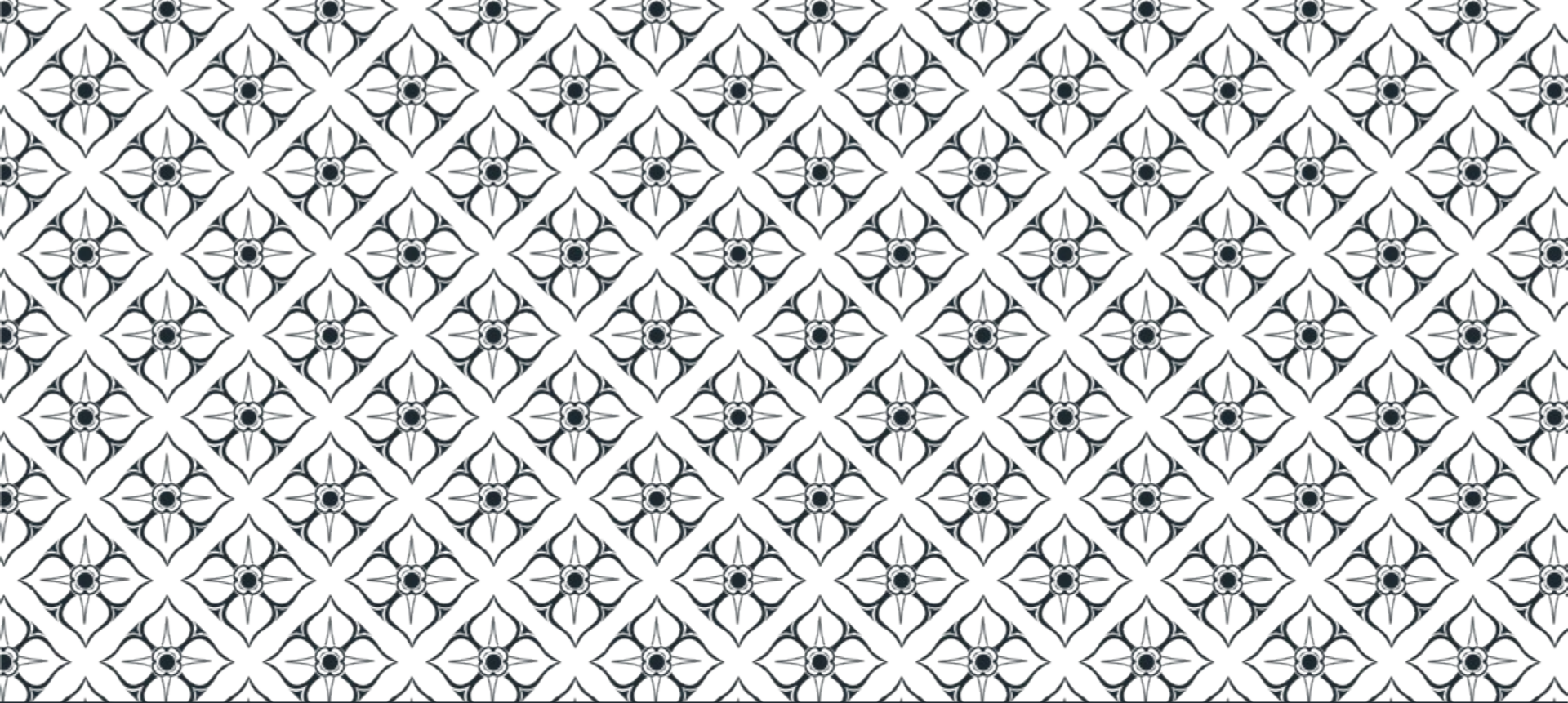


Charged Defects in ZnO



Charge ordering (with DFT+U)



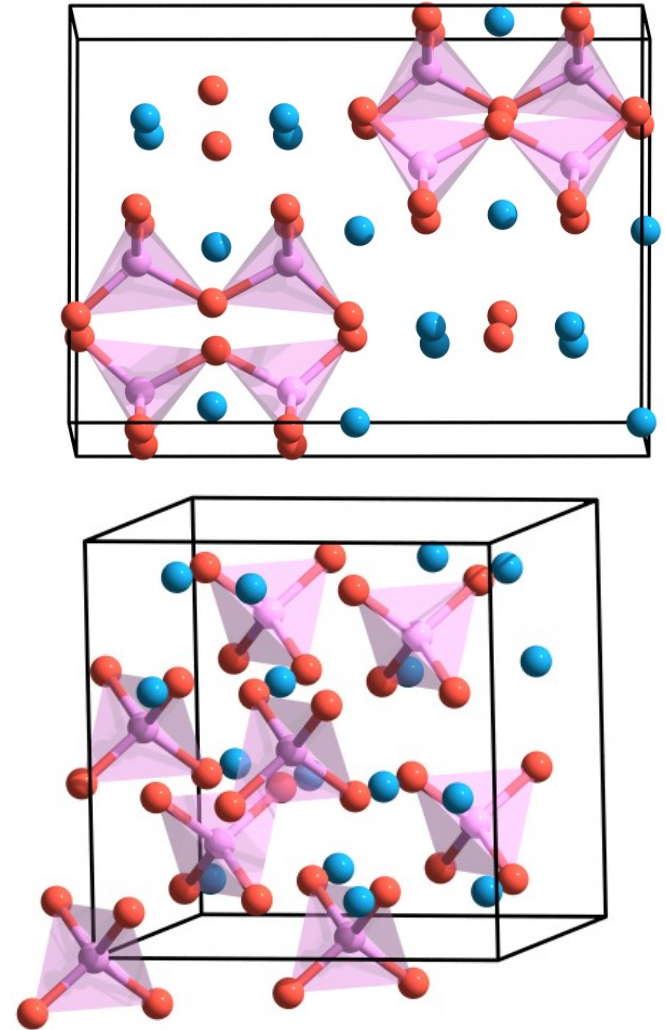
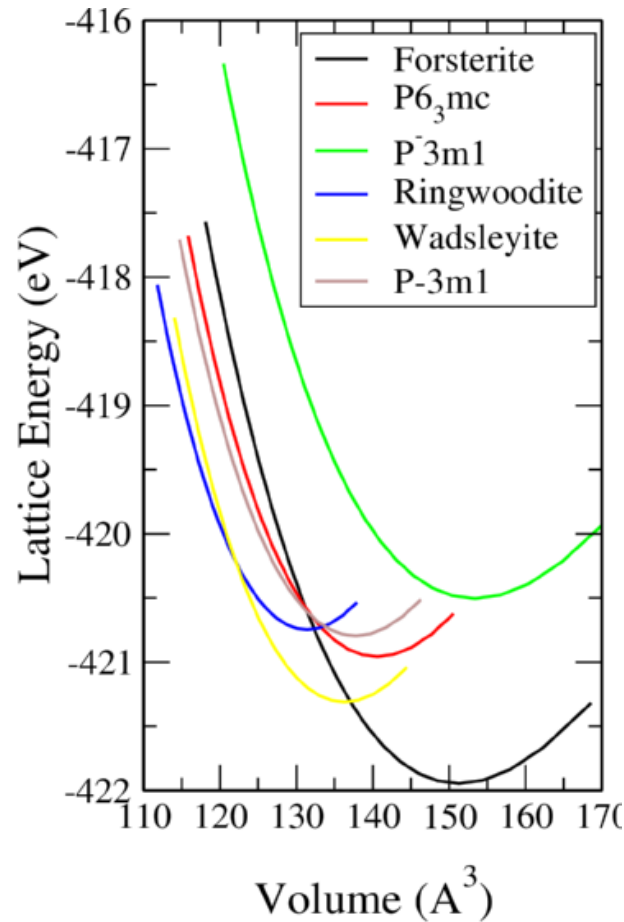
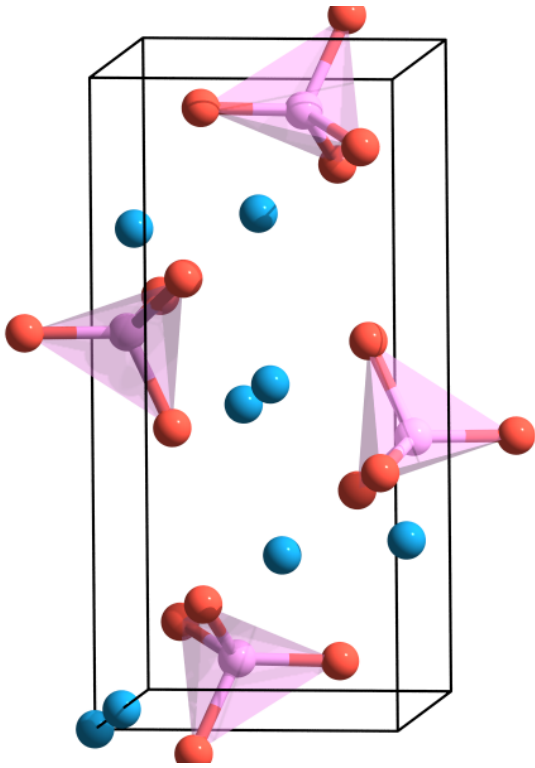


Crystal Structure

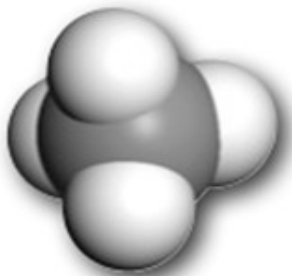
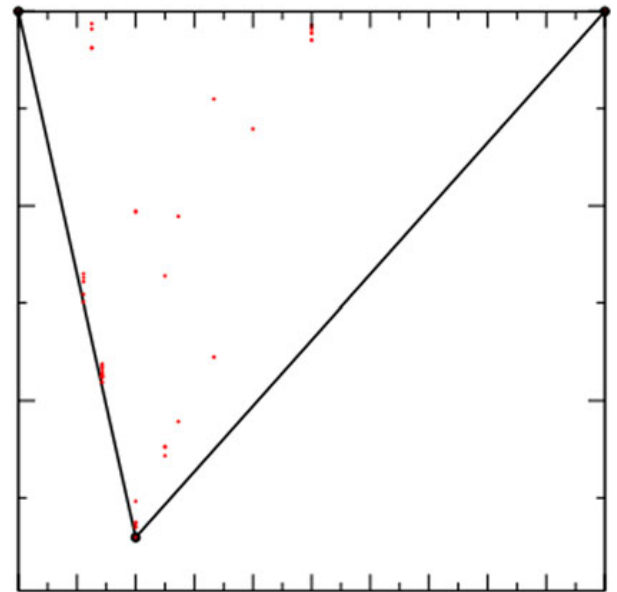
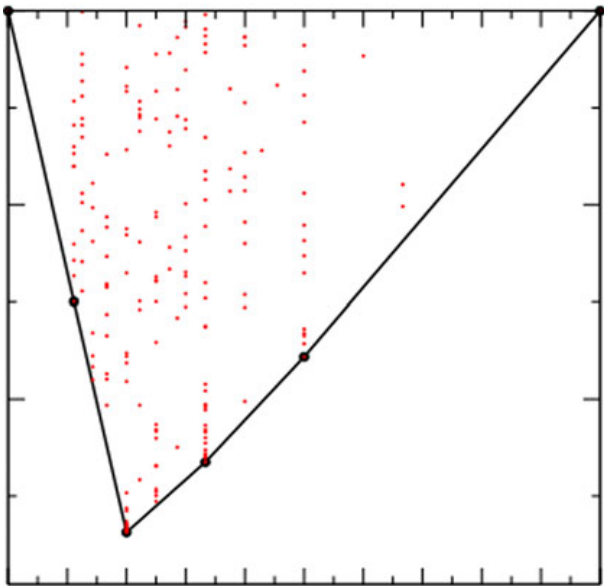


From electronic to crystal structure

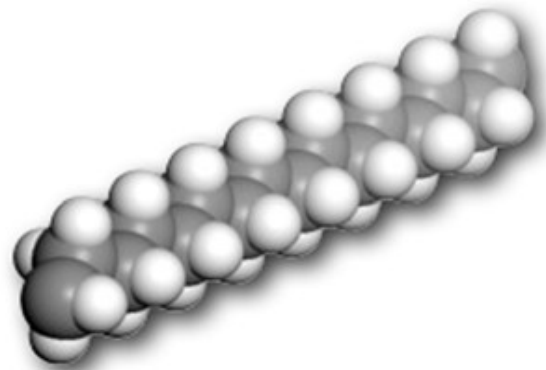
Polymorphs of Mg_2SiO_4



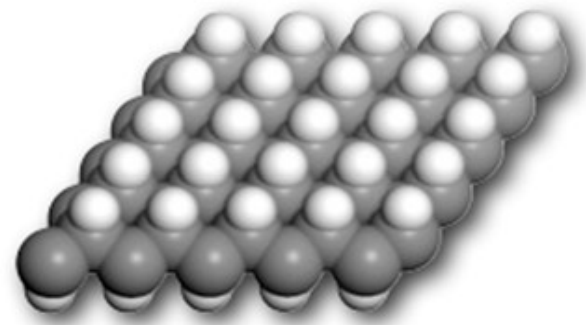
AIRSS: Prediction of Crystal Structures



methane

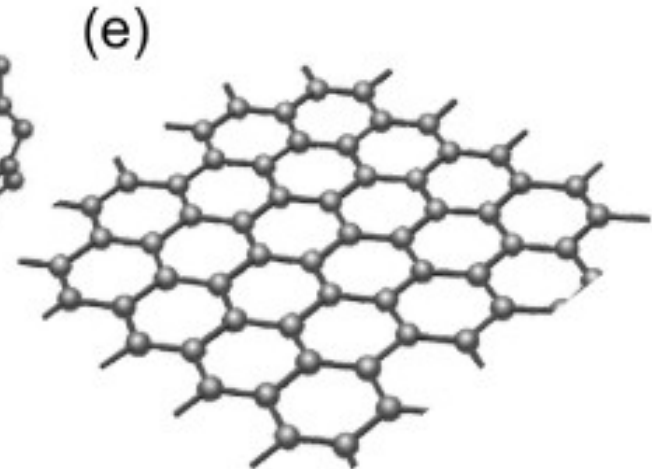
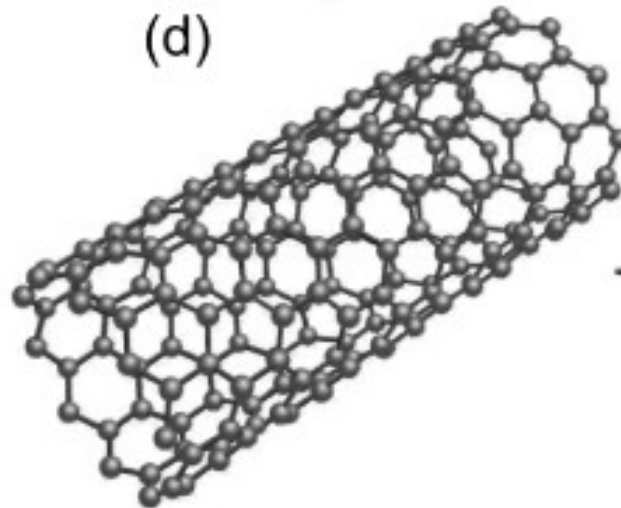
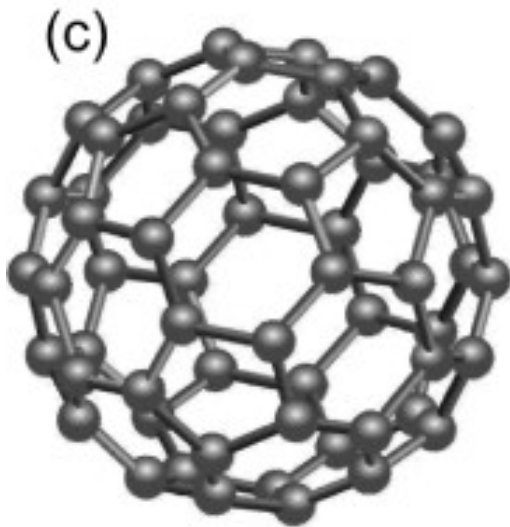
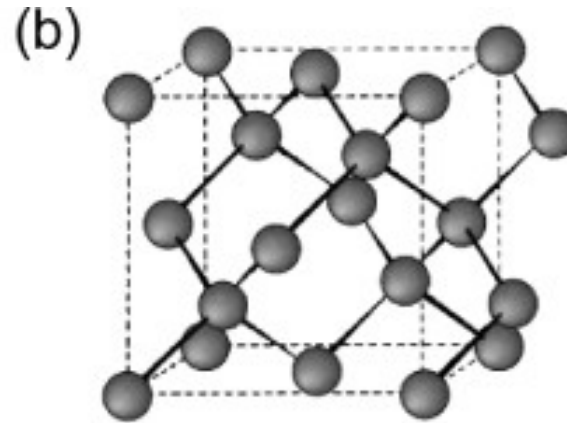
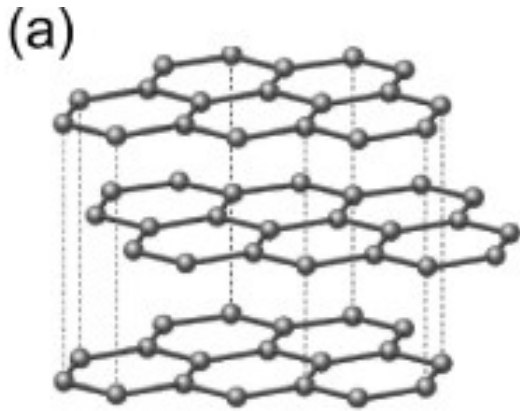


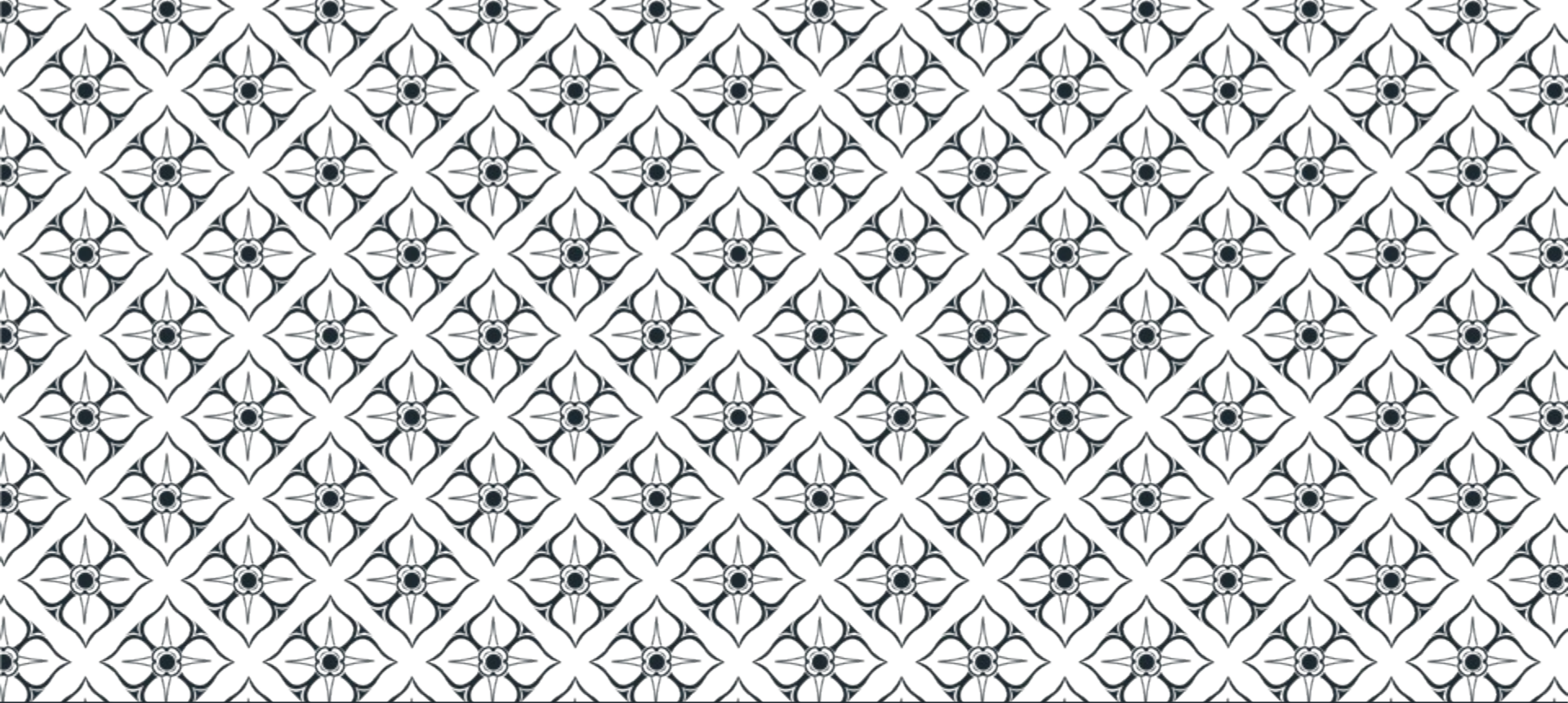
polyethane



graphane

Predicting Structure

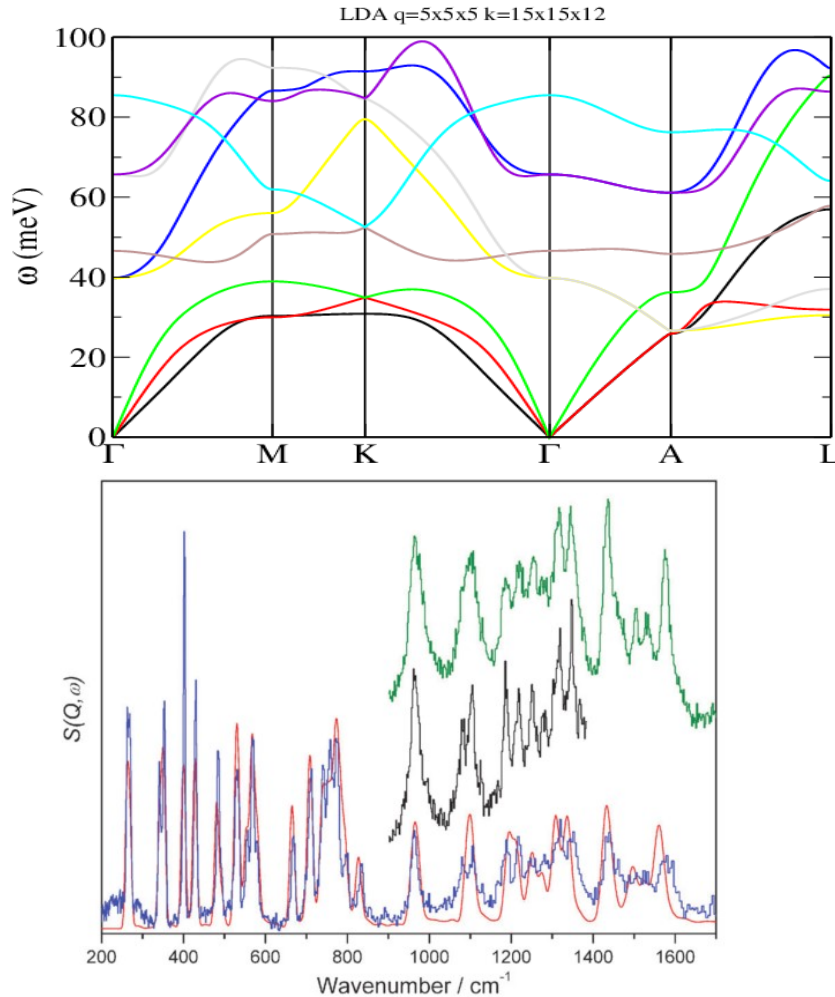




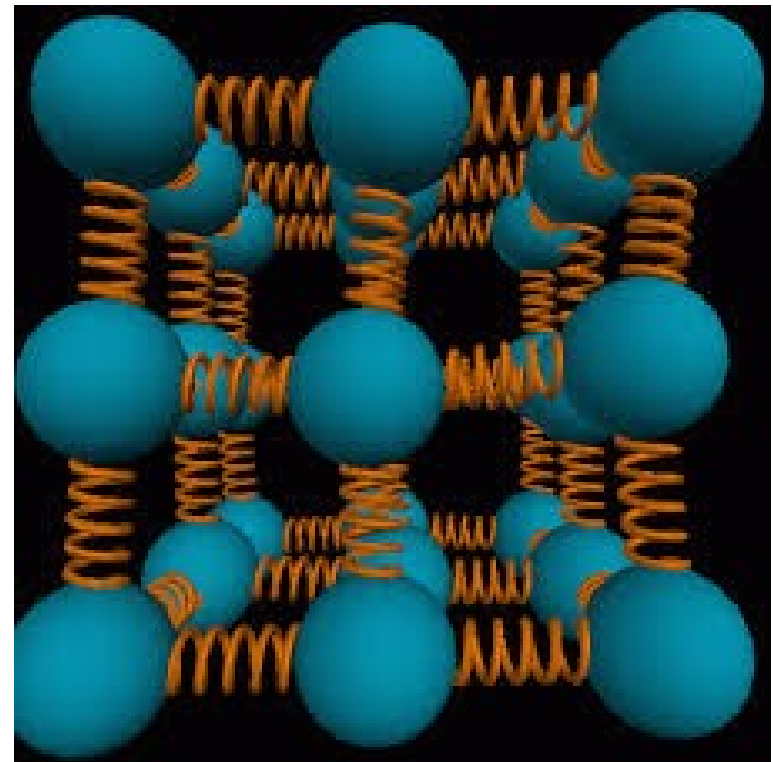
Vibrations, Phonons and Spectroscopy



Vibrational Spectroscopy



$$\Phi_{\kappa'\alpha'}^{\kappa\alpha}(\mathbf{0}, \mathbf{R}) = \frac{\partial^2 E}{\partial r_{\kappa\alpha} \partial r_{\kappa'\alpha'}}$$



Modelling the spectrum

Rotationally averaged infrared absorptivity

$$I_m = \left| \sum_{\kappa, b} \frac{1}{\sqrt{(M_\kappa)}} Z_{\kappa, a, b}^* u_{m, \kappa, b} \right|^2$$

Raman cross section

$$I_{\text{raman}}^m \propto |\mathbf{e}_i \cdot \mathbf{A}^m \cdot \mathbf{e}_s|^2 \frac{1}{\omega_m} \left(\frac{1}{\exp(\hbar \omega_m / k_B T) - 1} + 1 \right)$$

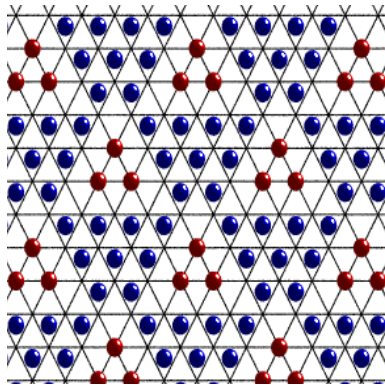
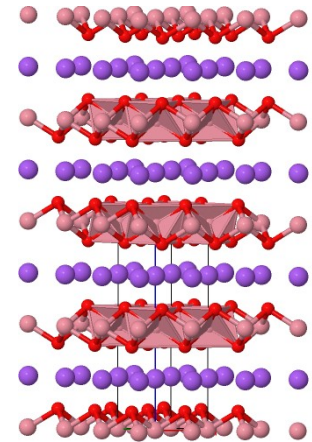
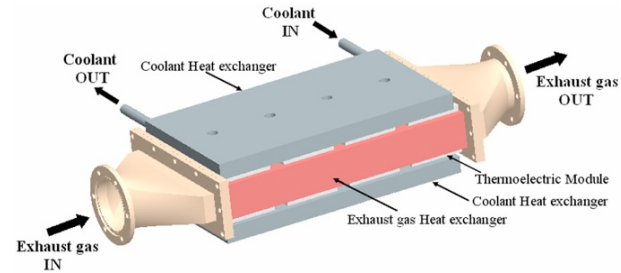
$$A_{\alpha, \beta}^m = \sum_{\kappa, \gamma} \frac{\partial^3 E}{\partial \epsilon_\alpha \partial \epsilon_\beta \partial u_{\kappa, \gamma}} u_{m, \kappa, \gamma} = \sum_{\kappa, \gamma} \frac{\partial \epsilon_{\alpha\beta}}{\partial u_{\kappa, \gamma}} u_{m, \kappa, \gamma}$$

Inelastic neutron cross section

$$S^n(\omega_m) = \int d\mathbf{Q} \sum_{\kappa} \sigma_{\kappa} \left\langle \frac{(Q \cdot u_{m, \kappa})^{2n}}{n!} \exp(-(Q \cdot u_{m, \kappa})^2) \right\rangle$$

Spectral response to light depends on response of **electrons**; for neutrons only **nuclei**.

Rattler mode in thermoelectric $\text{Na}_{0.8}\text{CoO}_2$

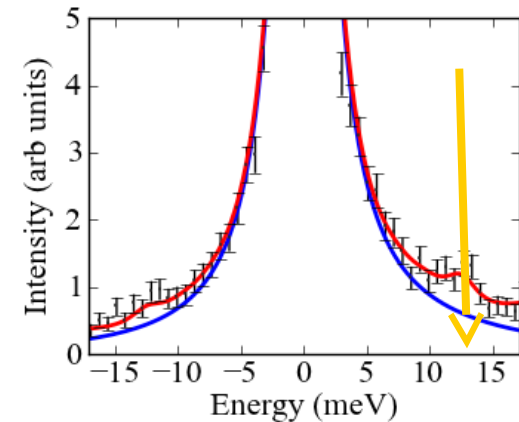


“Square Phase” Na ordering at 150K

Thermoelectric
“figure of merit”

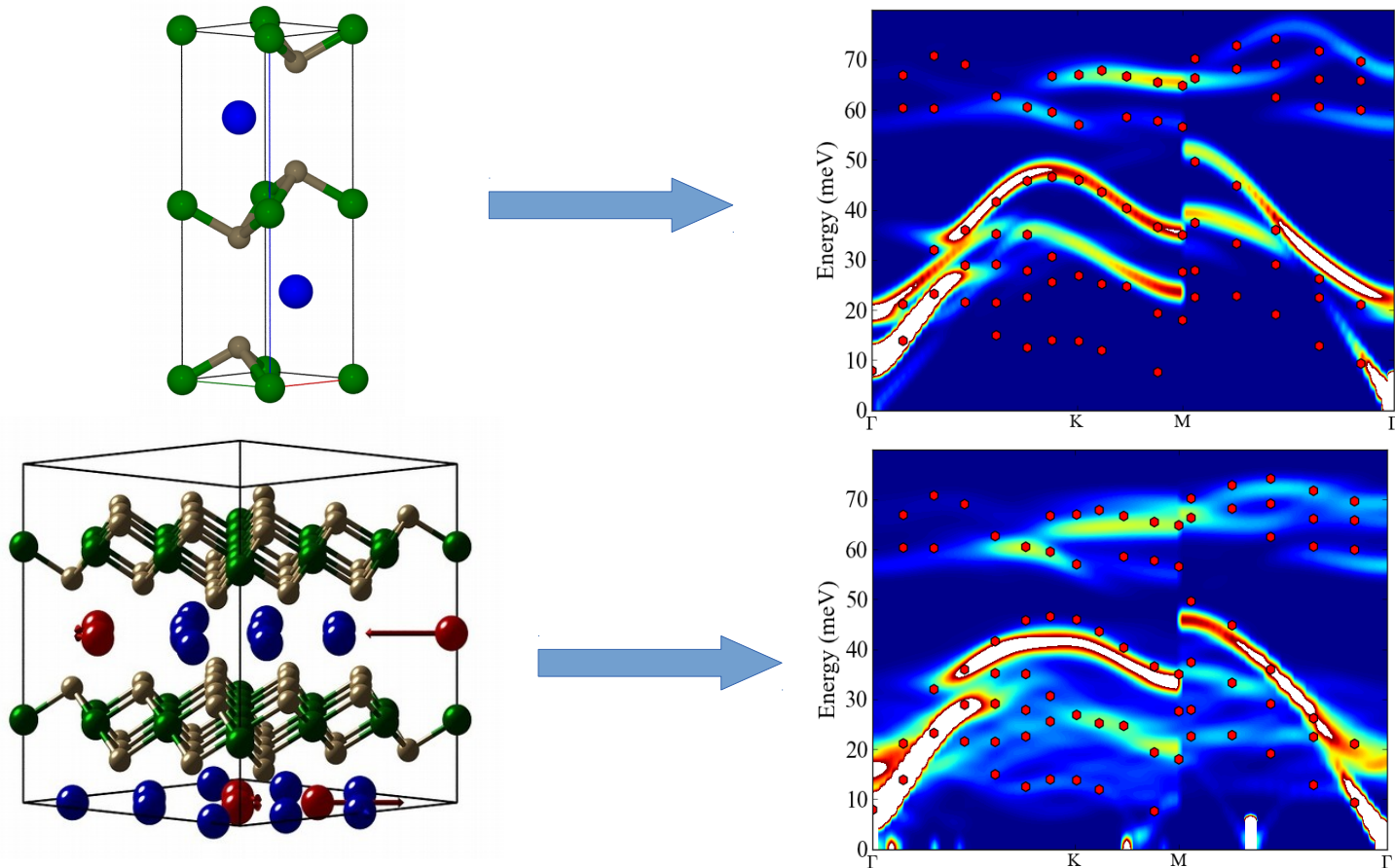
$$zT = \frac{S^2 T \sigma}{\kappa}$$

Roger, M., *et al.*, *Patterning of sodium ions and control of electrons in sodium cobaltate*. Nature **445**, 631 (2007)



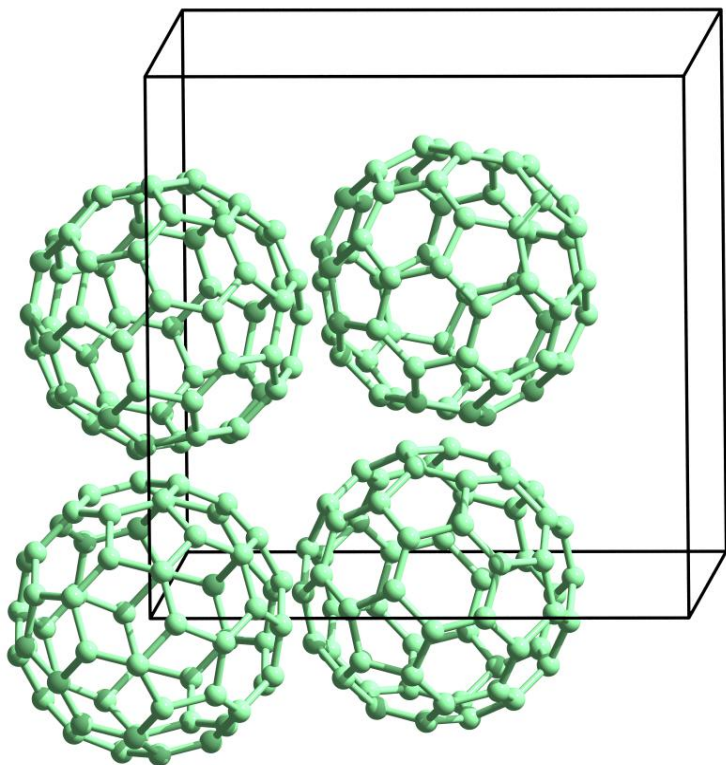
Inelastic X-Ray spectrum
measured at ESRF

Ab initio Lattice Dynamics



D. Voneshen et al., *Suppression of thermal conductivity by rattling modes in thermoelectric sodium cobaltate*. Nature Materials **12**, 1028 (2013)

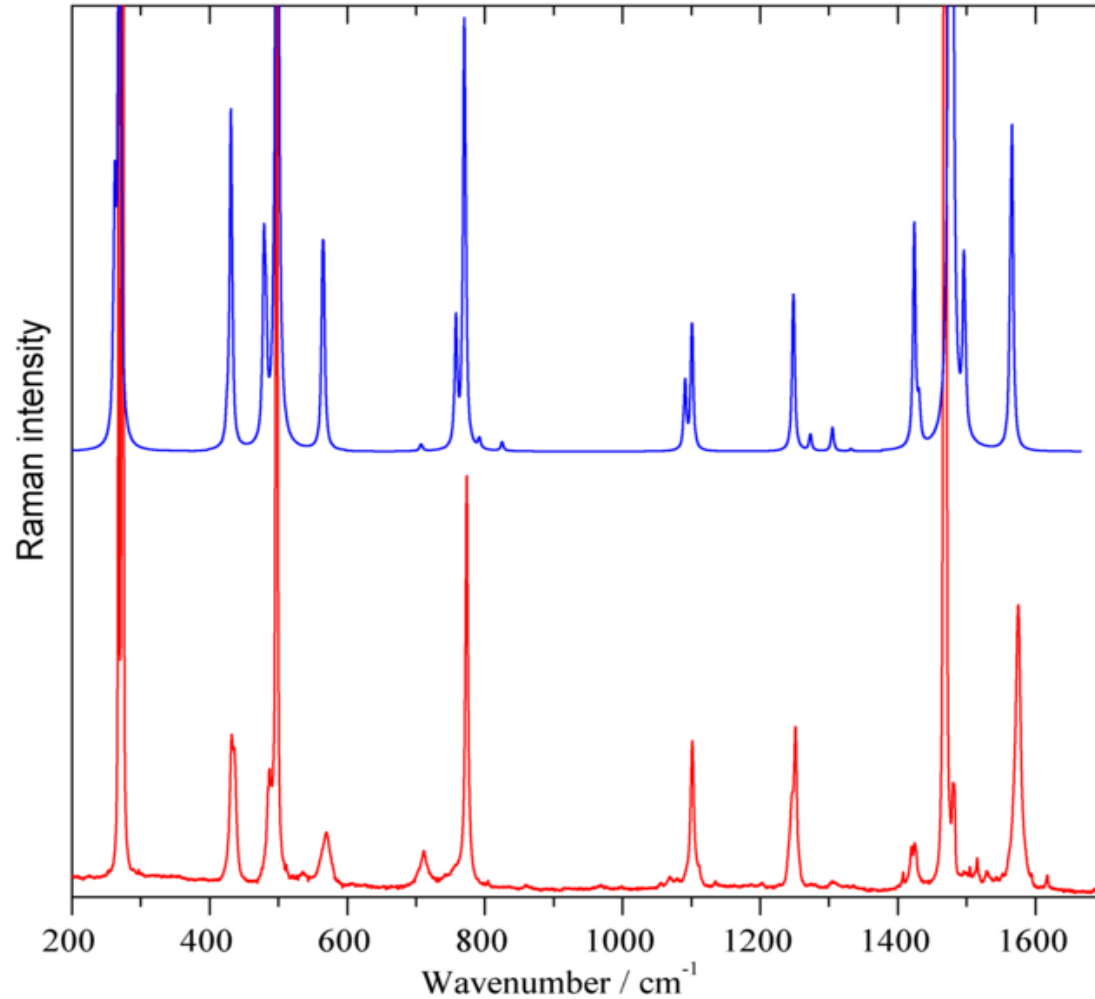
Vibrational spectroscopy of C_{60}



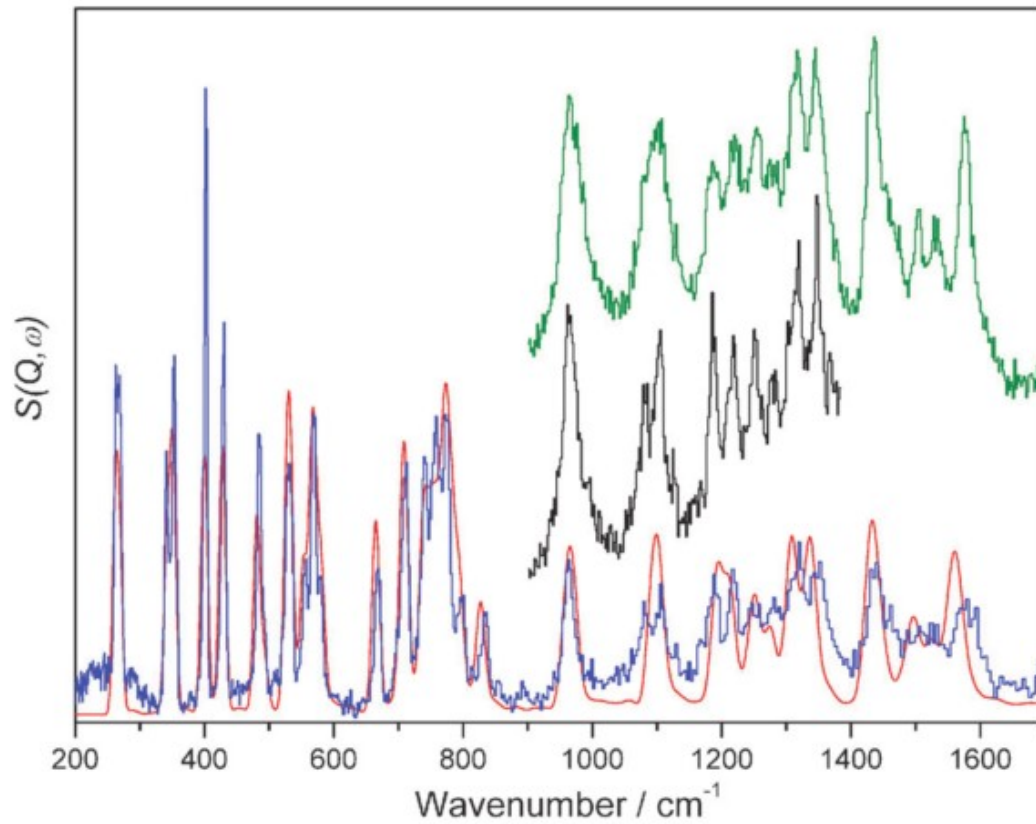
- Above 260K takes Fm3m structure with dynamical orientational disorder
- $m3m$ point group lower than I_h molecular symmetry
- Selection rules very different from gas-phase.
- Intramolecular modes and factor group splitting seen.
- Try ordered Fm3 model for crystal spectral calculation.

Parker et al, PCCP **13**, 7780 (2011)

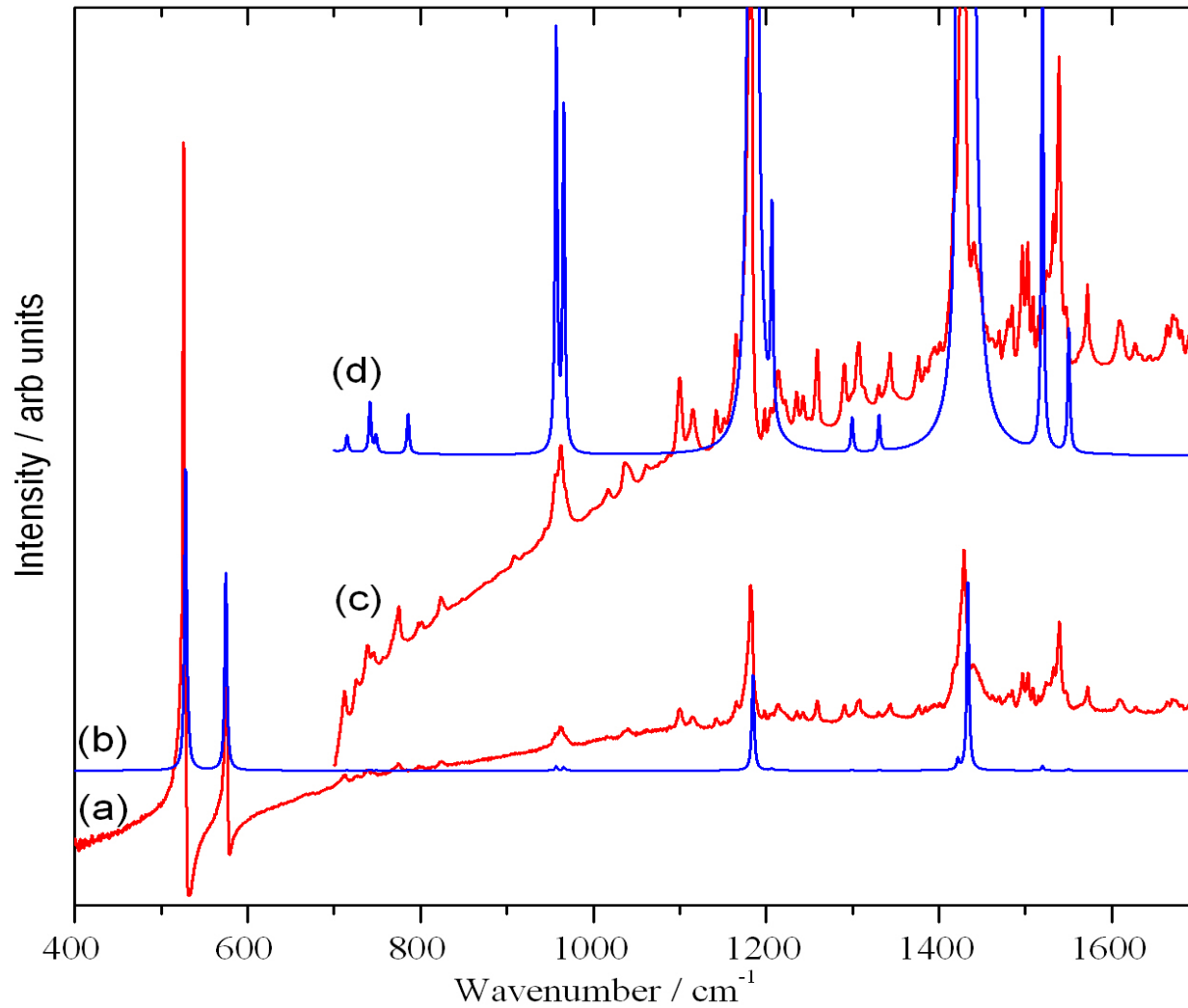
GGA Raman spectrum of C_{60}

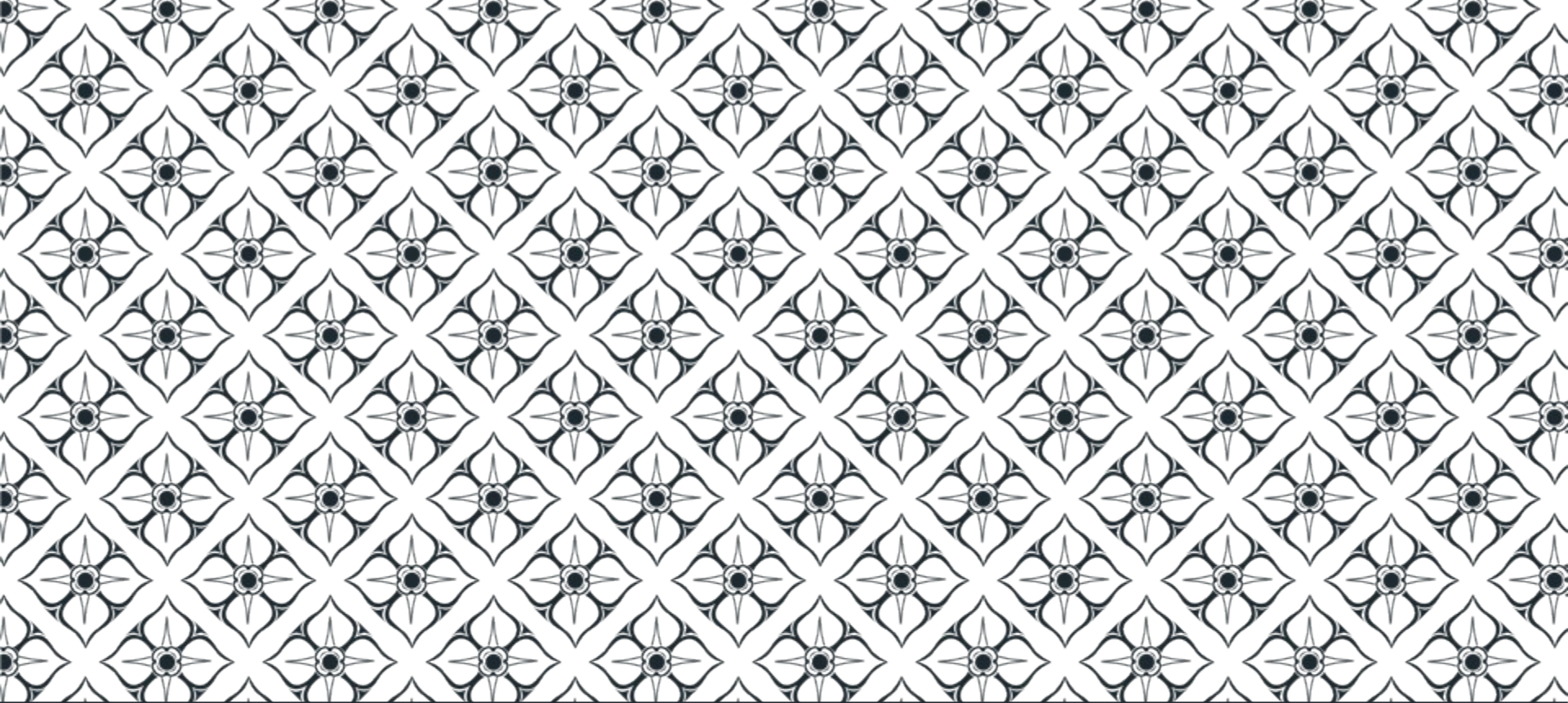


C₆₀ INS - Tosca



GGA infrared spectrum of C₆₀

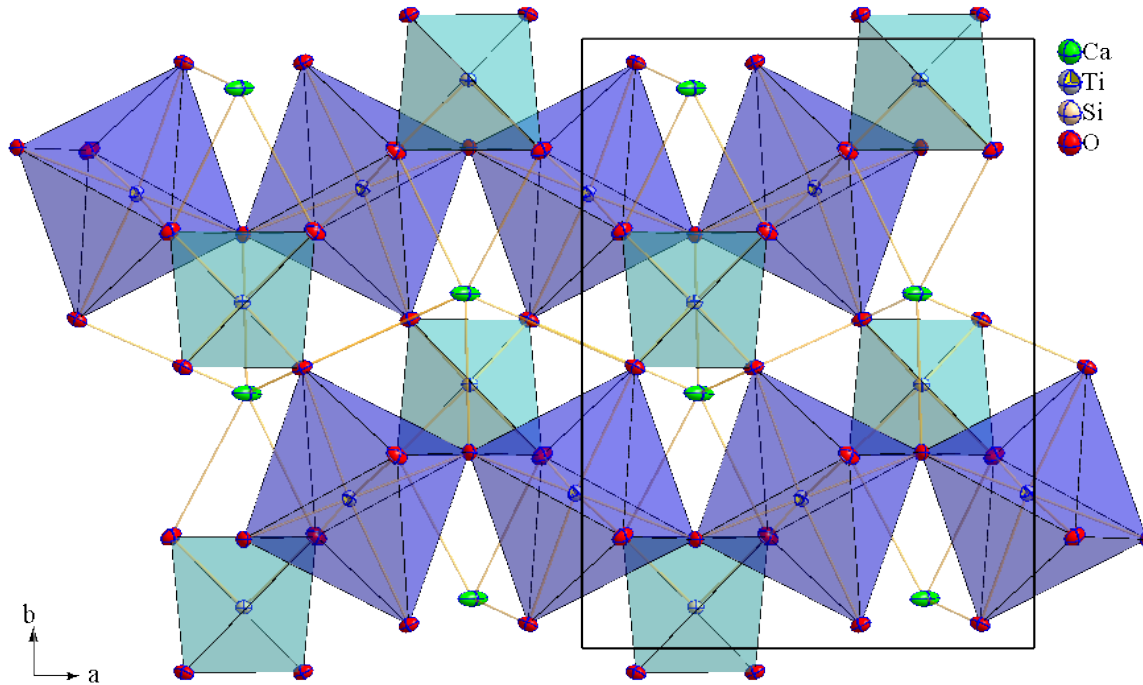




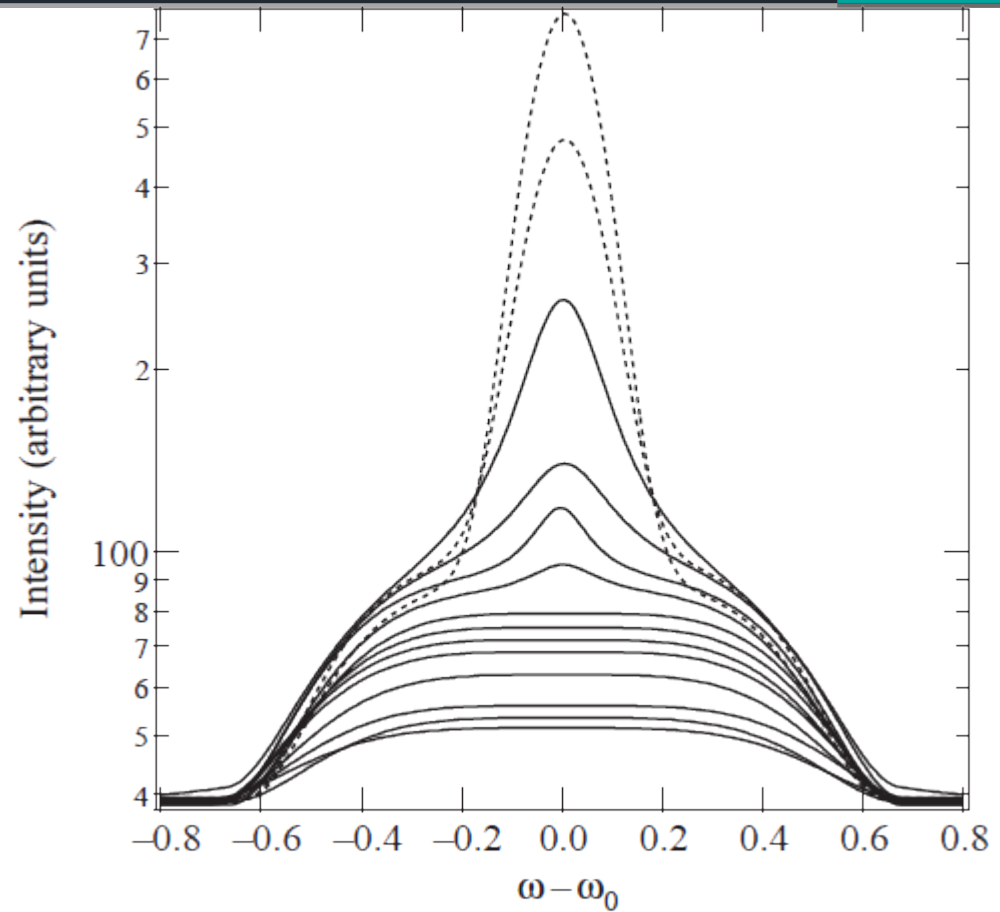
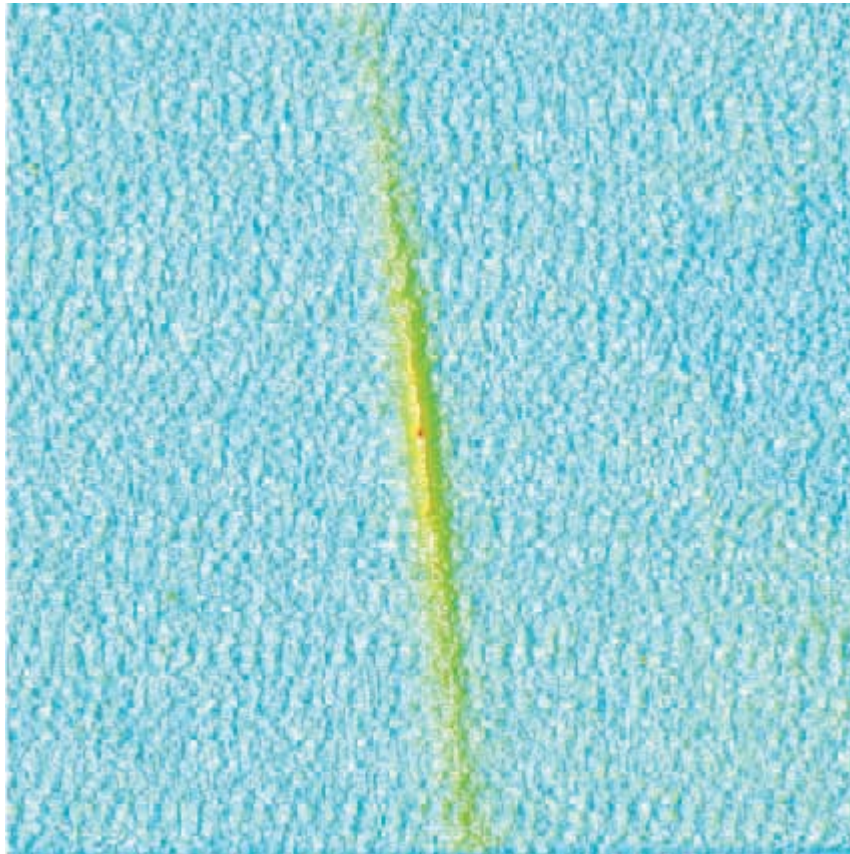
Phonons and Diffraction



Thermal Diffuse Scattering in Titanite



Motivation



Experiment



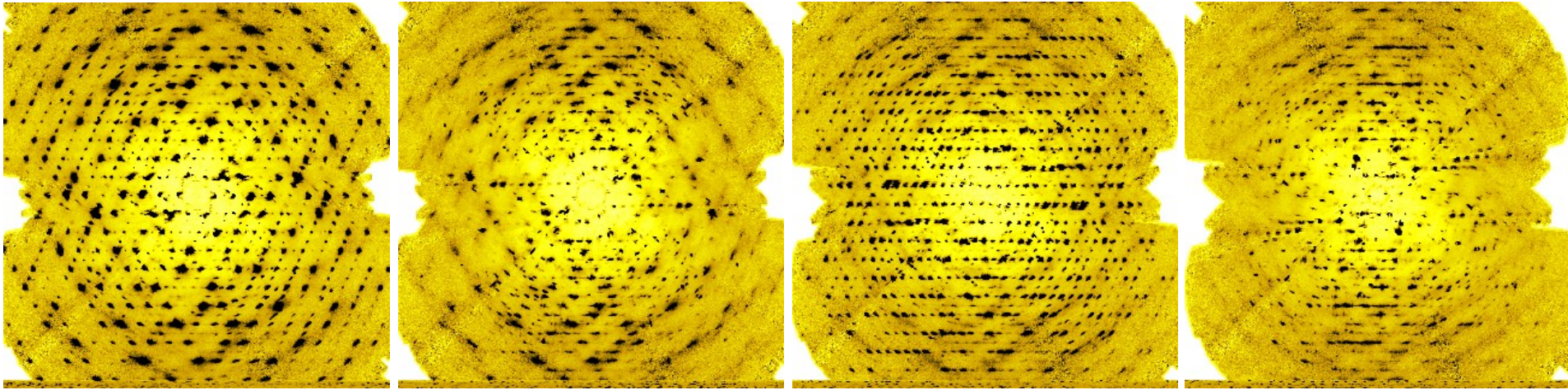
SXD at ISIS



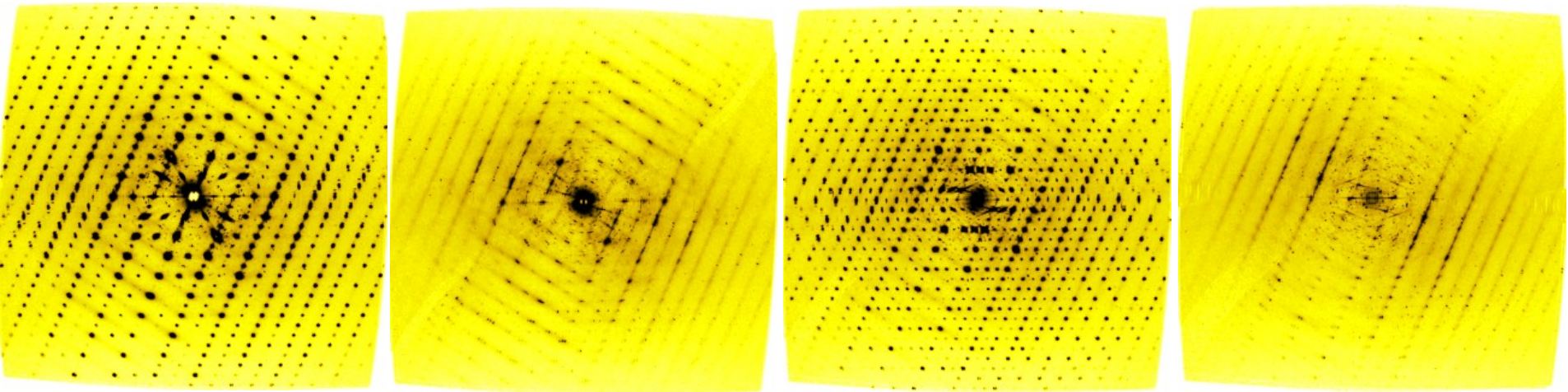
BW5 at DESY



Diffuse scattering



Neutron



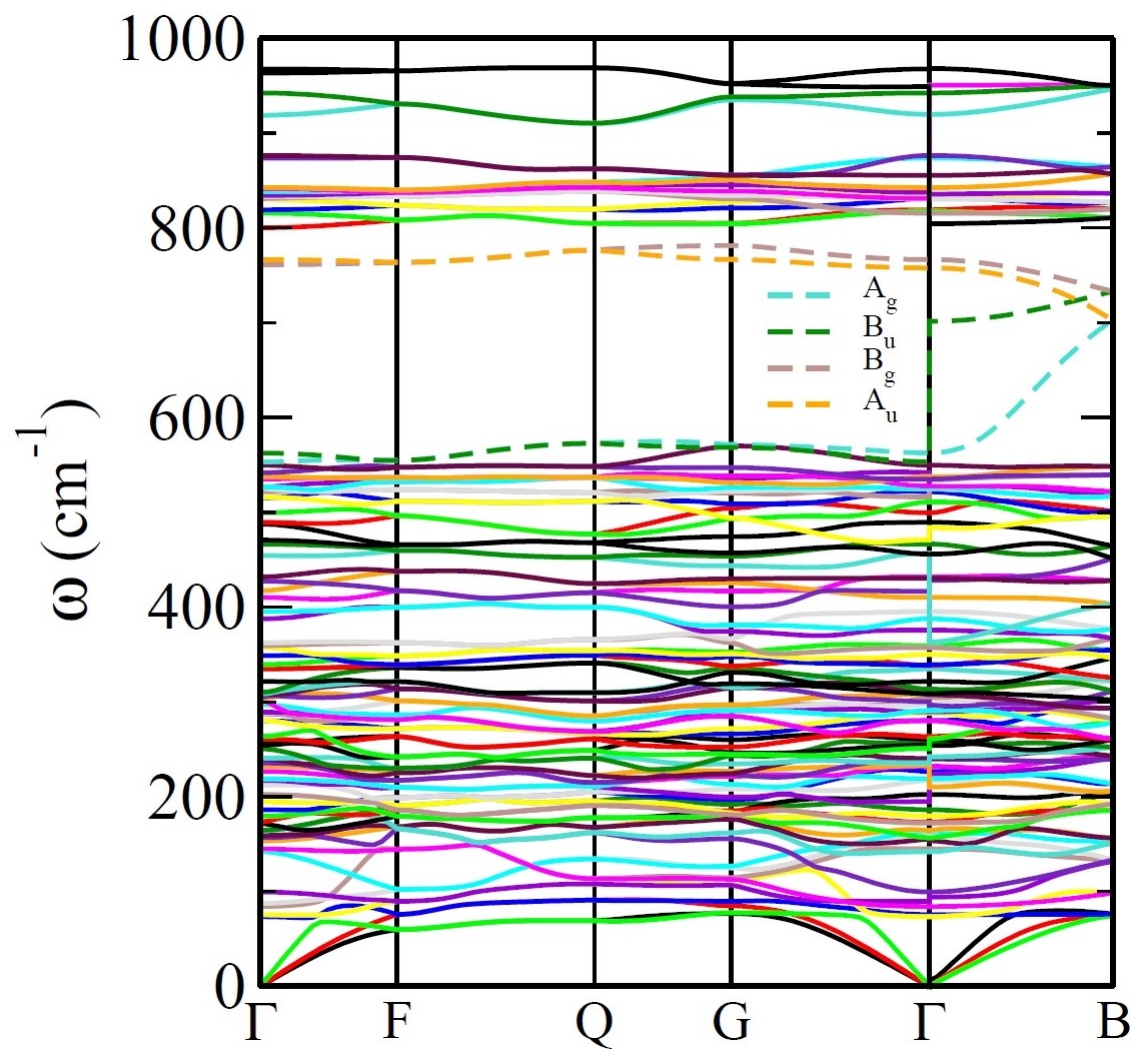
X-Ray

Phonons and diffraction

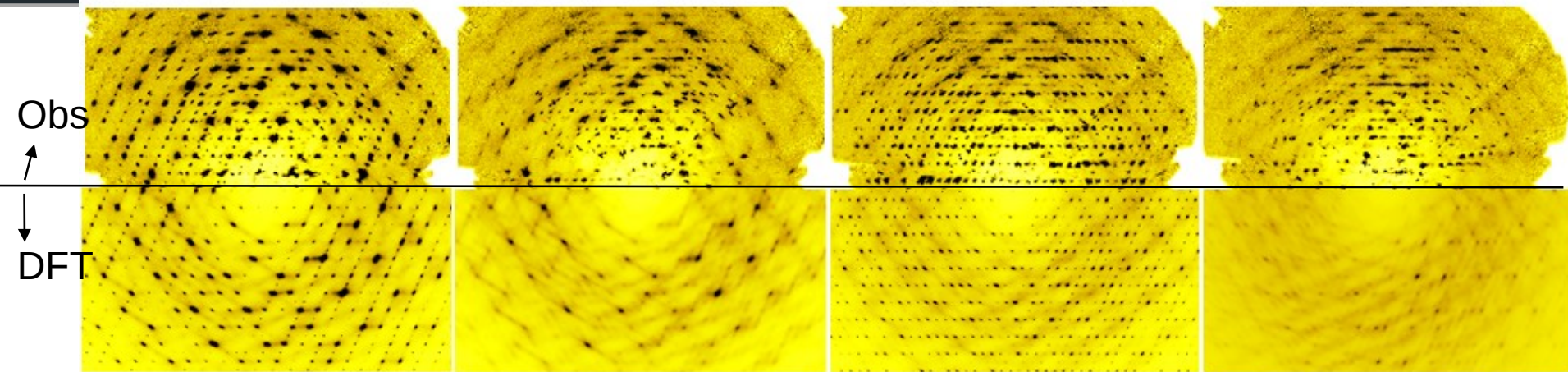
$$F_j(\vec{q}) = \sum_s \frac{f_s}{\sqrt{\mu_s}} \cdot e^{-M_s} \cdot (\vec{q} \cdot \vec{e}_{\vec{q},j,s}) \cdot e^{-i\vec{q} \cdot \vec{r}_s}$$

$$I_{TDS} = \frac{\hbar N I_e}{2} \sum_j \frac{1}{\omega_{\vec{q},j}} \coth\left(\frac{\hbar \omega_{\vec{q},j}}{k_B T}\right) |F_j(\vec{q})|^2$$

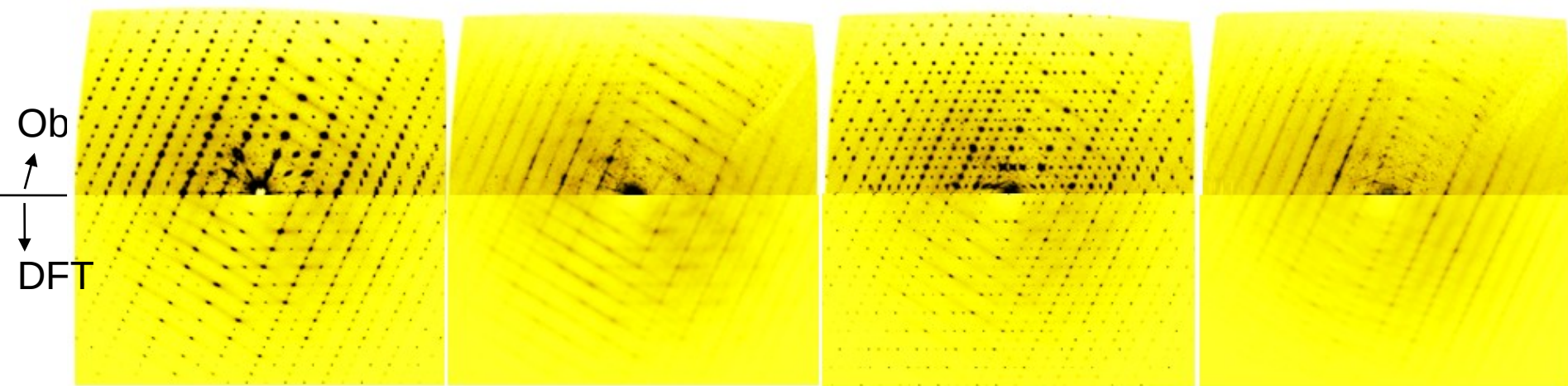
Dispersion curves from DFPT



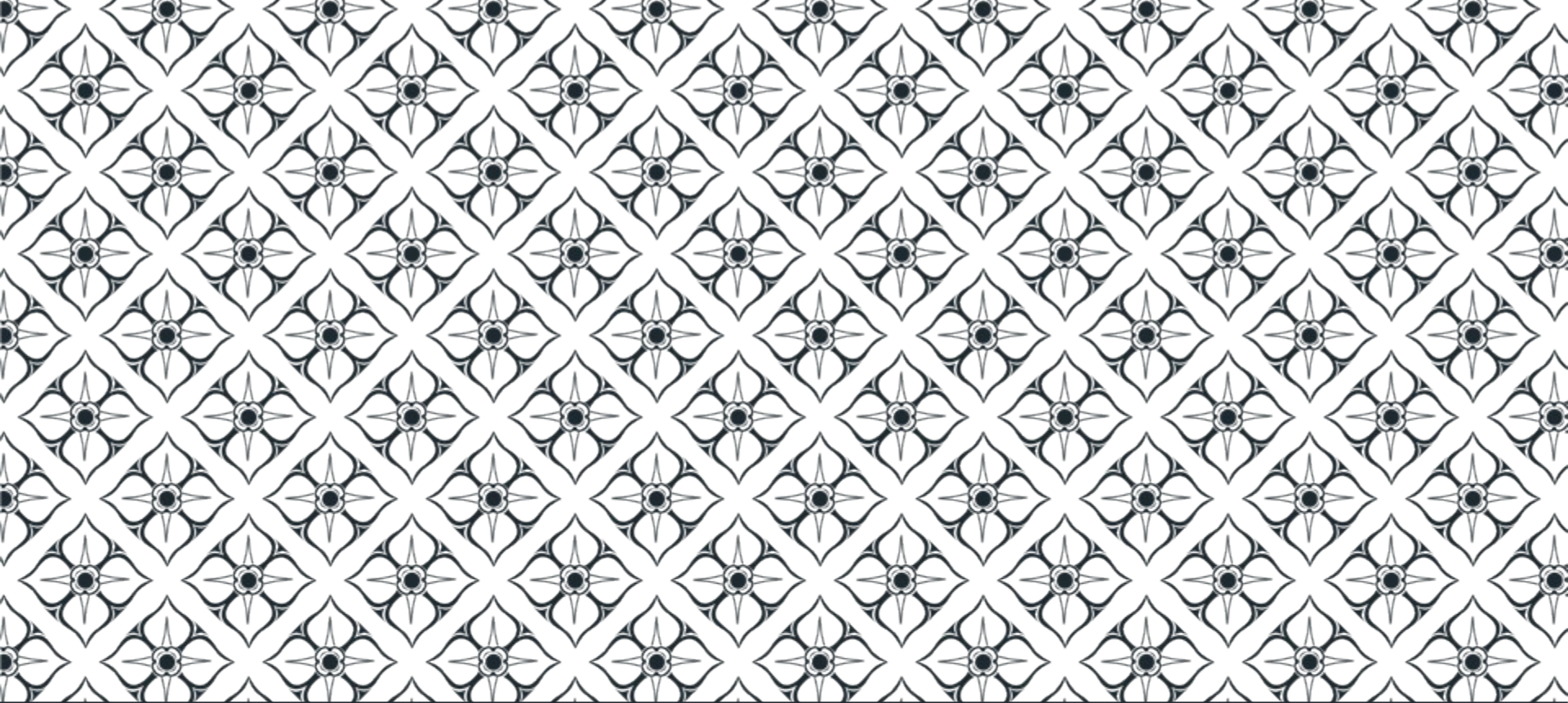
Comparison with data



Neutron



X-Ray



Dynamics and Dynamic Structure



Dynamics of nuclei

With forces calculated from DFT

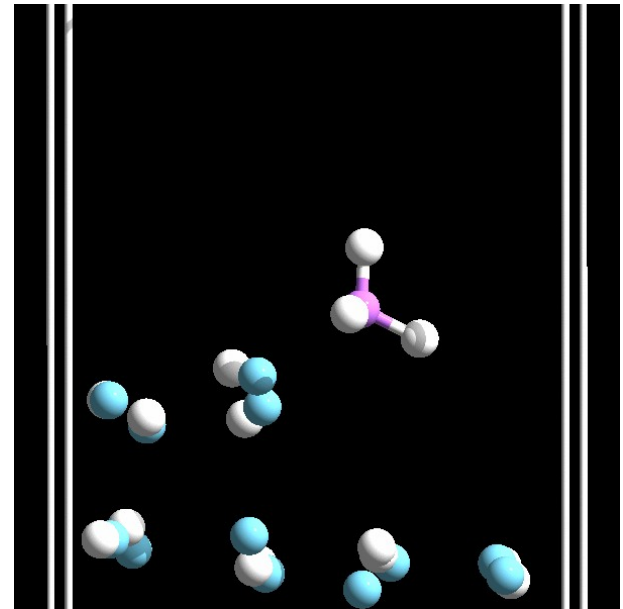
Can also calculate **dynamics**:

- Molecular dynamics – time evolution
- Lattice dynamics - spectroscopy

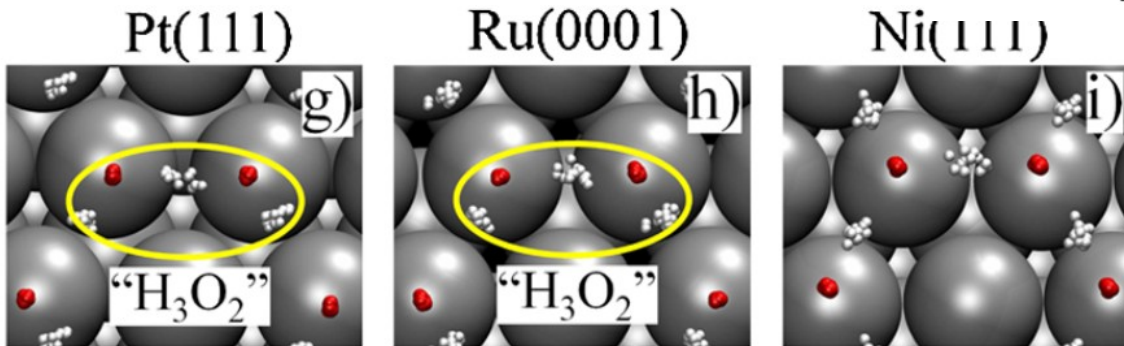
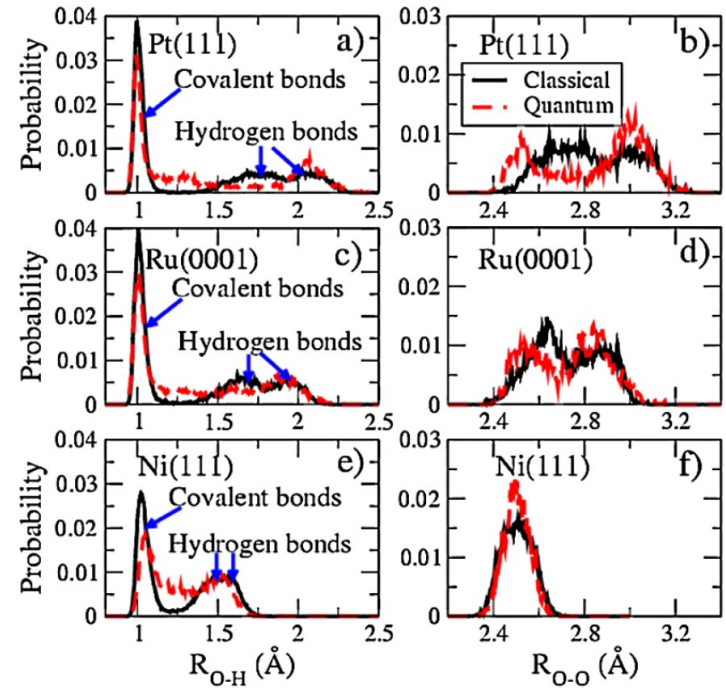
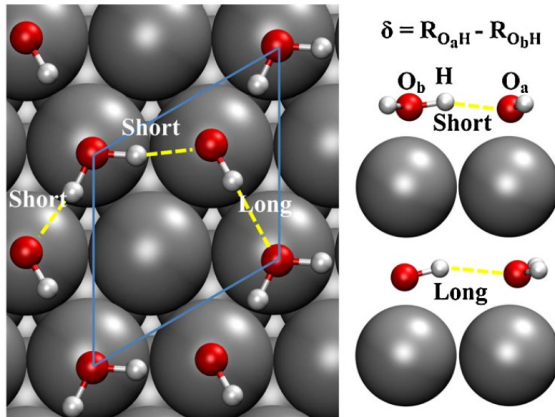
$$r(t + \delta t) = r(t) + v(t)\delta t + \frac{1}{2}a(t)\delta t^2$$

$$v(t + \delta t) = v(t) + \frac{1}{2}[a(t) + a(t + \delta t)]\delta t$$

$$a(t + \delta t) = \frac{1}{m}F(t + \delta t)$$



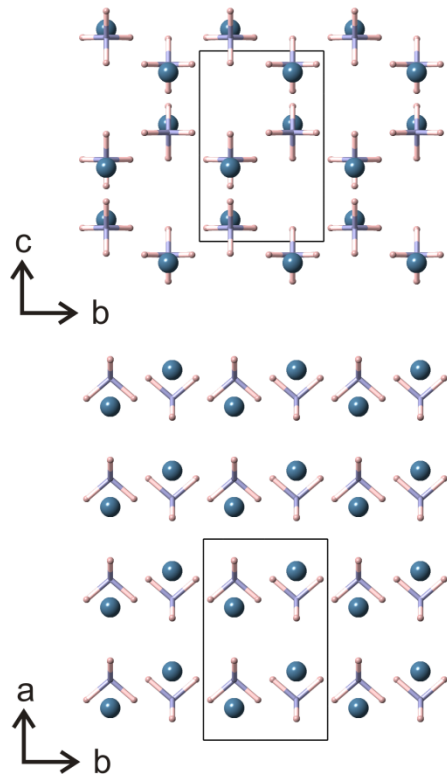
Water on metal Surfaces



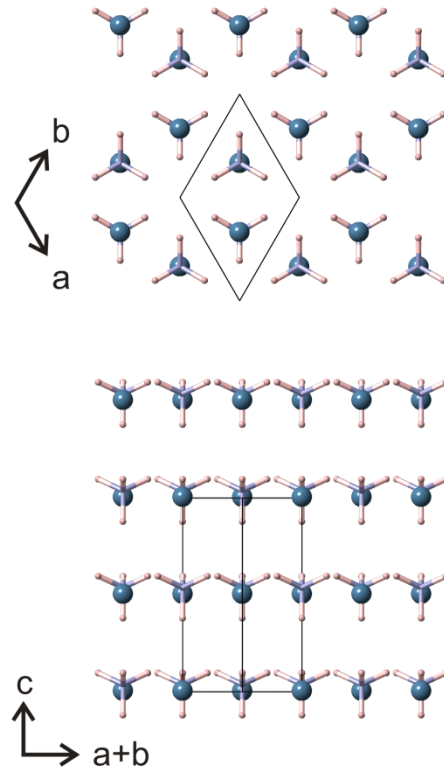


Superionic conductivity in LiBH_4

Fast-ion conduction in LiBH_4



< 390 K
Orthorhombic (Pnma)

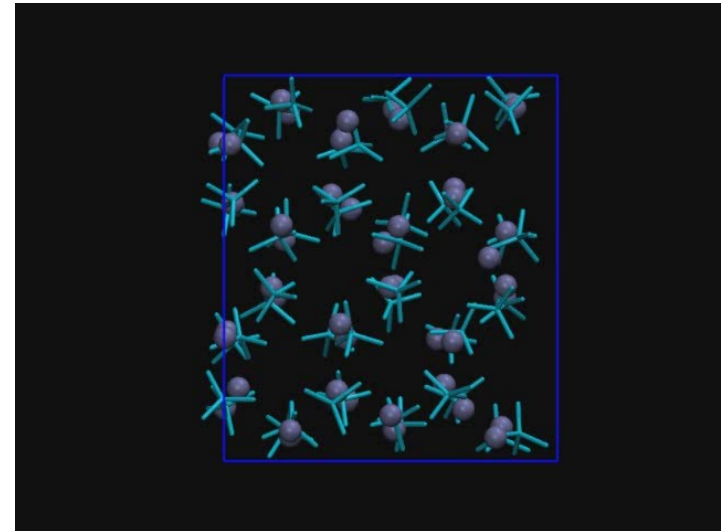


> 390 K
Hexagonal (P63/mmc)
Disordered
Superionic conductivity

> 560 K: liquid
> 650 K: decomposition

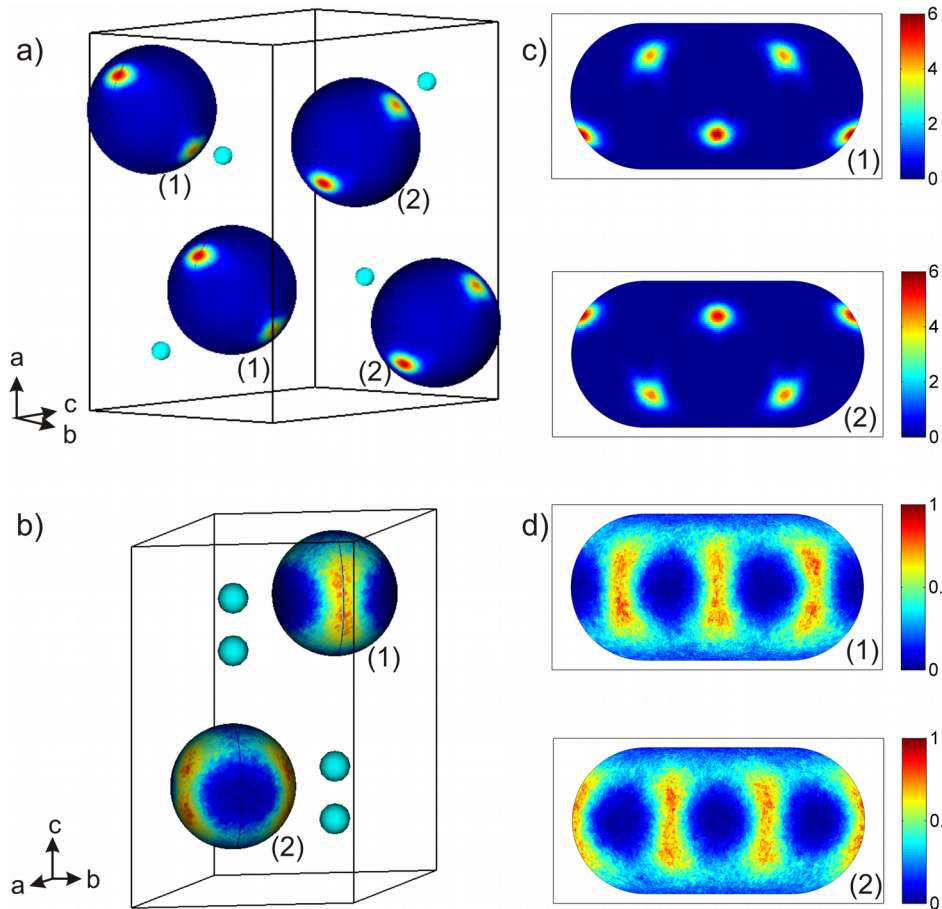
Ab Initio Molecular Dynamics

- Code: CP2K
- Born-Oppenheimer molecular dynamics in isokinetic ensemble (Gaussian thermostat)
- Forces evaluated by DFT using the QUICKSTEP method
- Supercell: 288 atoms (48 formula units)
- Time step: 0.5 fs
- Run lengths 20-30 ps after equilibration
- PBE exchange-correlation functional
- Dual basis set (Gaussian DZ orbitals & plane waves up to 280 Ry) and Goedecker pseudopotentials are used



Equilibrium MD picture

BH4 rotational disorder:

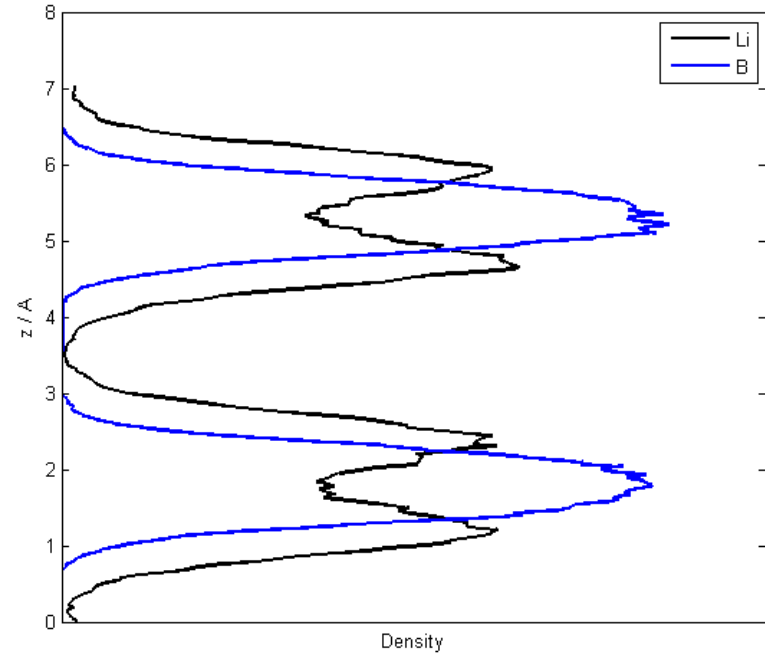
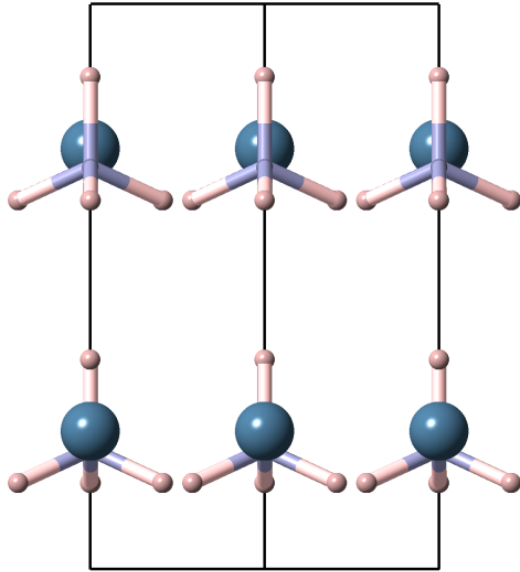


298K

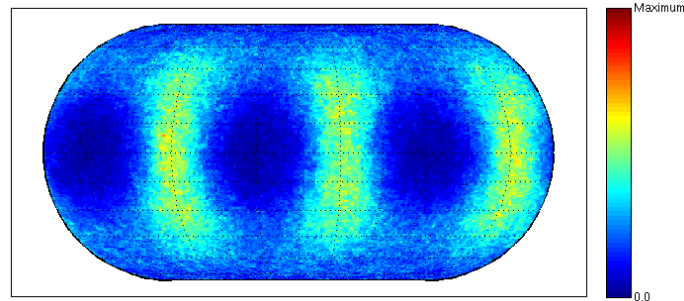
473K

Equilibrium MD picture

Li dynamical disorder:

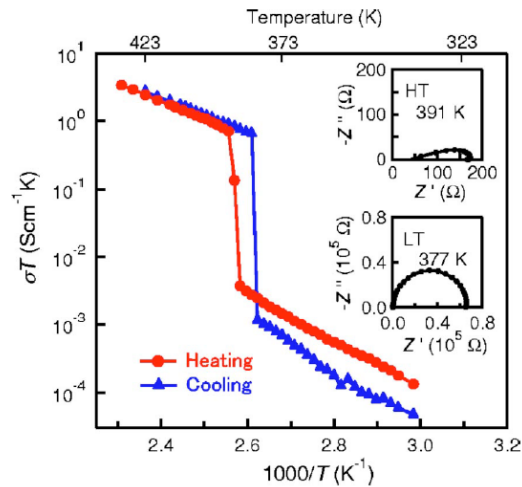


BH4 rotational disorder:

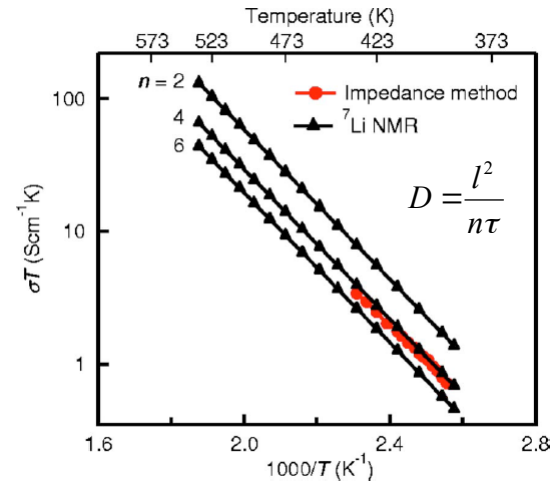


Measurements of Li mobility

Motoaki Matsuo et al., Applied Physics Letters **91**, 224103 (2007).



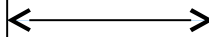
A/C impedance measurements



Li-7 NMR measurements

At 535K:

$$\sigma = 0.139 \text{ S/cm}$$



$$D_{\text{Li}} = 2.28 \cdot 10^{-6} \text{ cm}^2/\text{s}$$

Calculating diffusion by AIMD

Diffusion coefficient calculated by...

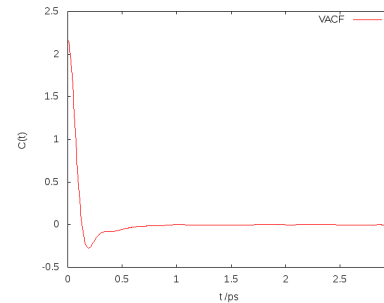
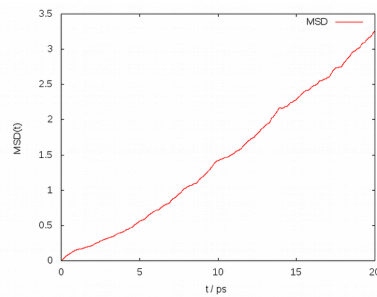
Einstein-Sutherland equation

$$D = \frac{1}{n} \frac{d\langle r^2(t) \rangle}{dt}$$

Green-Kubo formula

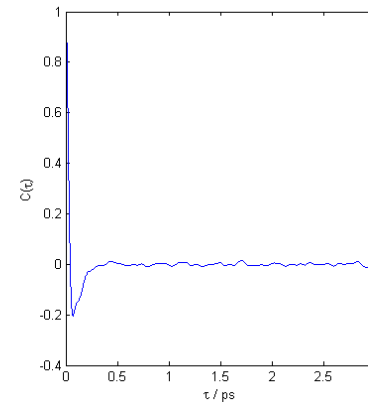
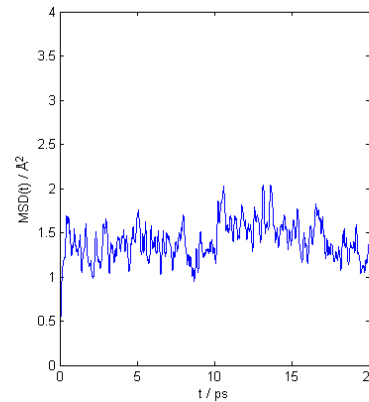
$$D = \frac{2}{n} \int_0^{\infty} dt \langle v(0) \cdot v(t) \rangle$$

Lennard-Jonesium
(mimicking liquid Argon)



Fast diffusion

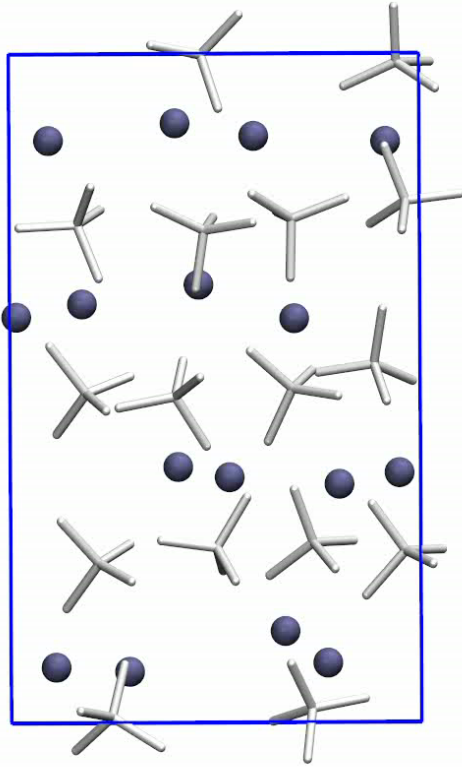
LiBH4 at 535 K



Diffusion by ion jumps
(rare events)
which are often
followed by a jump back
to the original position

Limits of AIMD: diffusion in fluids with $D > 10^{-5} \text{ cm}^2/\text{s}$

Nonequilibrium Molecular Dynamics



- An external field \mathbf{F}_e is applied that couples to a fictitious atomic property (“colour”, c_i):

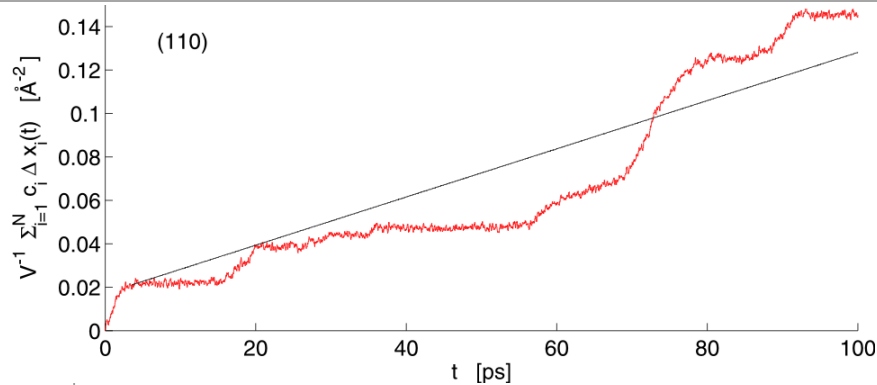
$$\dot{\mathbf{p}}_i = \mathbf{F}_i + c_i \mathbf{F}_e$$

- The (fictitious) field and its induced response are related by (real) transport coefficients:

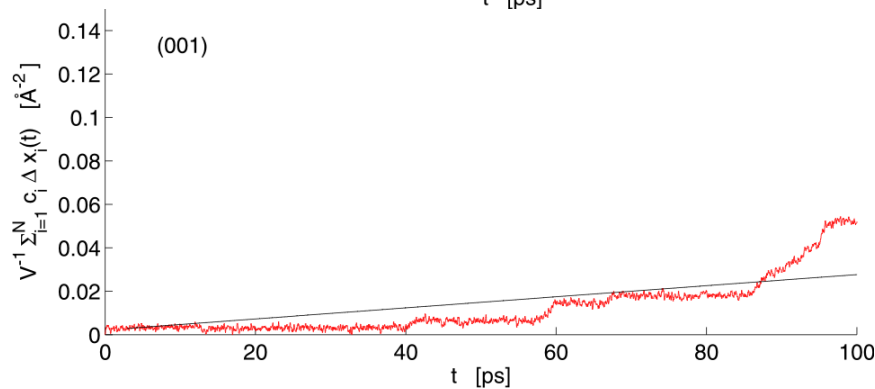
$$D = \frac{k_B T}{\rho_c} \lim_{t \rightarrow \infty} \lim_{F_e \rightarrow 0} \frac{\langle J_c(t) \rangle}{F_e}$$

- NEMD functionality implemented in CASTEP and CP2K
- *ab initio* nature of the method allows mechanism discovery

Results – $F_e = 0.05 \text{ eV/\AA}$

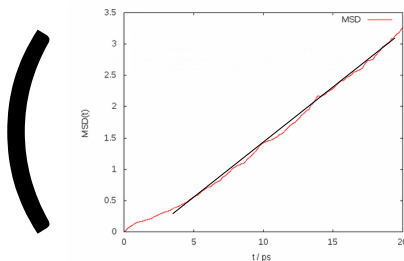


$$D_{\text{Li}} = 5.82 \cdot 10^{-6} \text{ cm}^2/\text{s}$$



$$D_{\text{Li}} = 1.34 \cdot 10^{-6} \text{ cm}^2/\text{s}$$

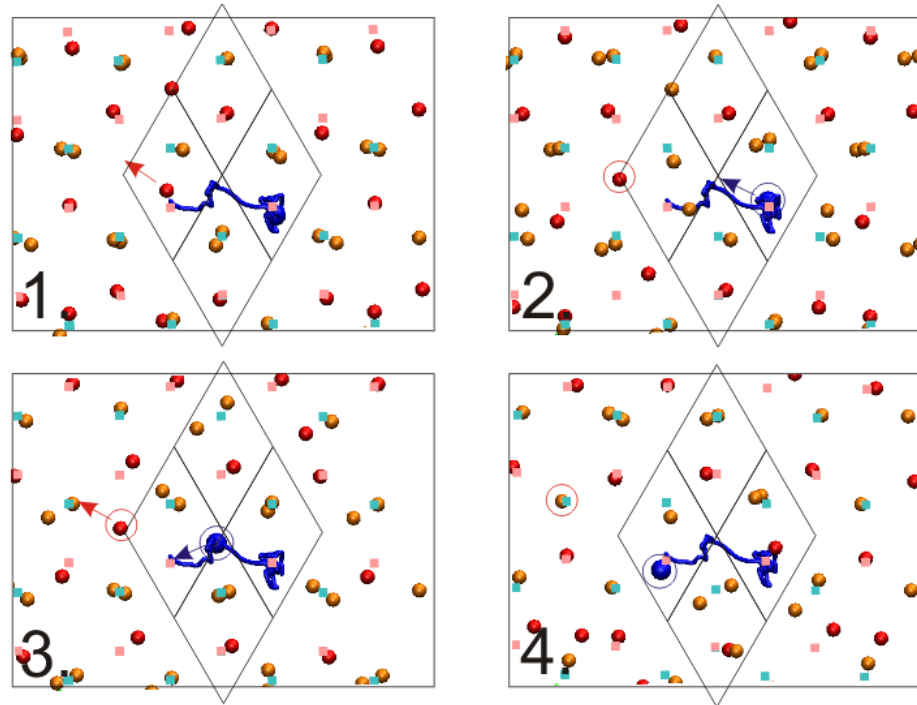
(Measured: $D_{\text{Li}} = 2.28 \cdot 10^{-6} \text{ cm}^2/\text{s}$)



Compare: $D = \frac{1}{n} \frac{d\langle r^2(t) \rangle}{dt}$ vs $D = \frac{k_B T}{\rho_c} \lim_{t \rightarrow \infty} \lim_{F_e \rightarrow 0} \frac{\langle J_c(t) \rangle}{F_e}$

Diffusion Pathway

Inspection of the NEMD trajectory:



hopping is via jumps from a lattice site into an empty interstitial site (2 & 3),
and from there on to another lattice site (4).

P.C. Aeberhard, S. Williams, D. Evans, K. Refson, and W.I.F. David, *Physical Review Letters* 108, 095901 (2012).

The Nature of BH_4^- Reorientations in Hexagonal LiBH_4

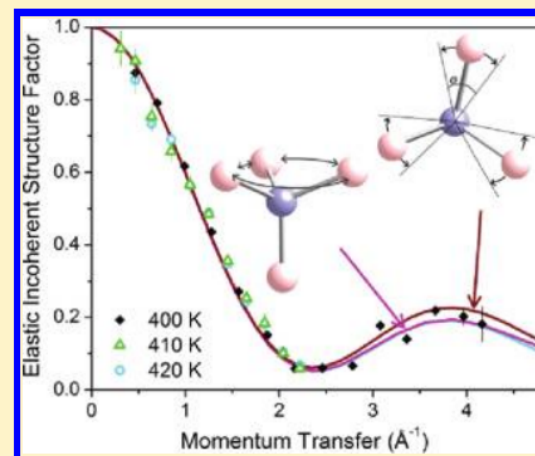
Nina Verdal,^{*,†} Terrence J. Udovic,[†] and John J. Rush^{†,‡}

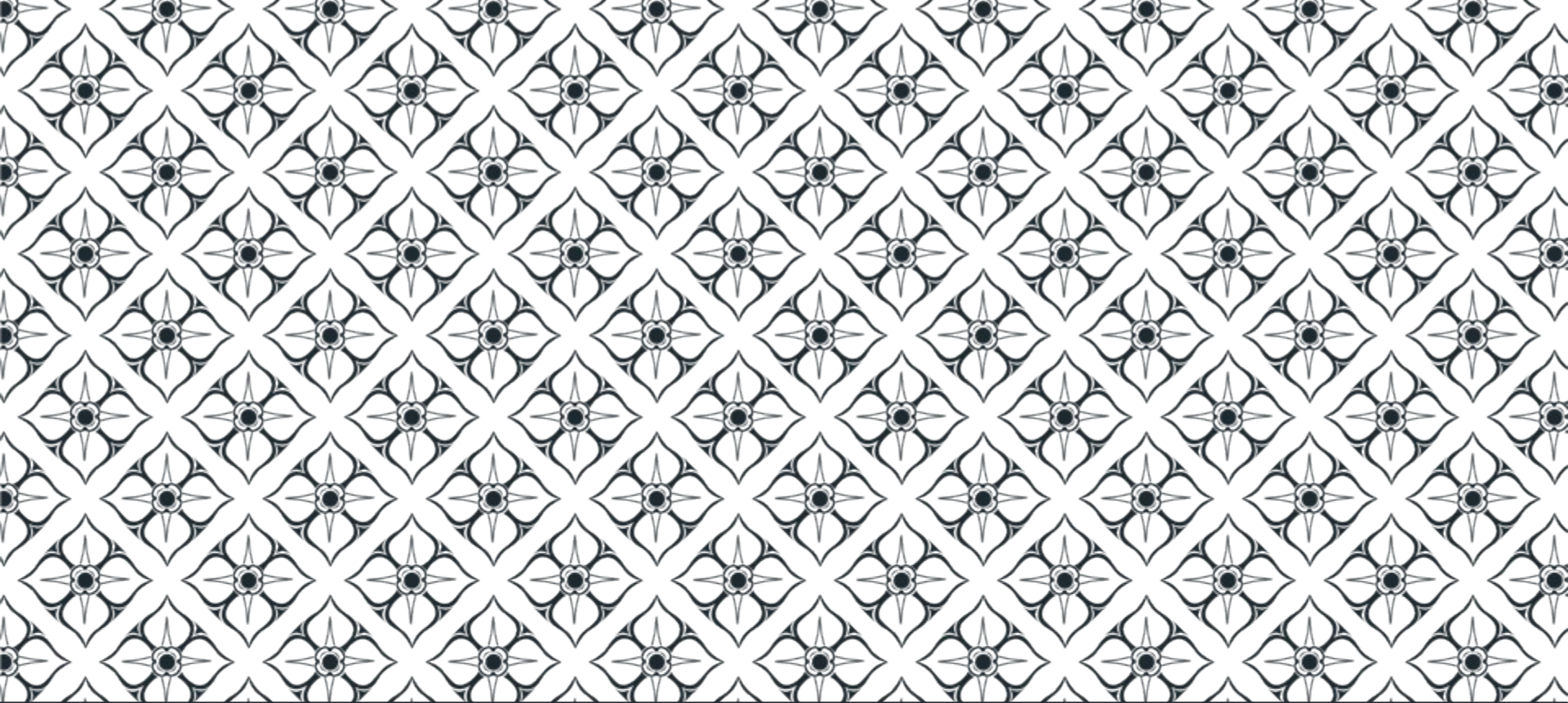
[†]NIST Center for Neutron Research, National Institute of Standards and Technology, 100 Bureau Dr., MS 6102, Gaithersburg, Maryland 20899-6102, United States

[‡]Department of Materials Science and Engineering, University of Maryland, 2135 Chemical & Nuclear Engineering Bldg., College Park, Maryland 20742-2115, United States

S Supporting Information

ABSTRACT: Lithium borohydride (LiBH_4) has lately been the subject of intense inquiry within the hydrogen storage community. Quasi-elastic neutron scattering spectra were measured for LiBH_4 in the high-temperature hexagonal crystal phase. The elastic incoherent structure factor associated with the rapid BH_4^- anion reorientations was determined at 400, 410, and 420 K for momentum transfers as high as 4.2 \AA^{-1} . The results strongly suggest a BH_4^- reorientational mechanism approaching quasi-free, trigonal-axis rotation of three borohydride H atoms, combined with reorientational jump exchanges between these delocalized “orbiting” H atoms and the remaining axial borohydride H atom. This mechanism is consistent with previously reported diffraction and spectroscopy studies.





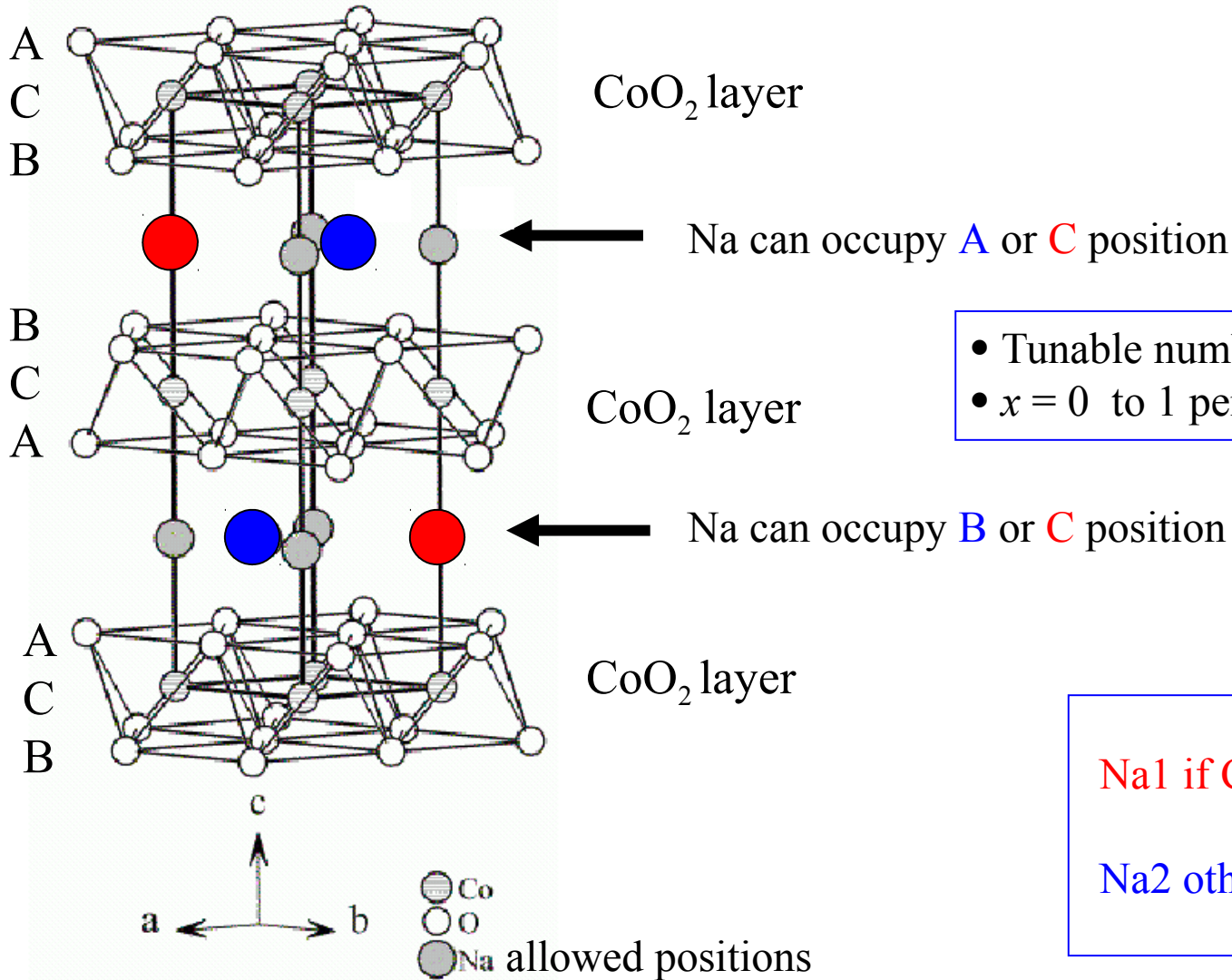
Na_xCoO_2 again- Na-ion Batteries



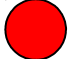
Na-ion batteries

- Expanding use of Li-ion batteries into new areas of energy storage:
- High-capacity and large-scale deployment?
 - Automotive
 - Load-levelling for renewable energy
- Problem Li is *scarce* and *expensive*
- *Large-scale deployment for high-capacity poses significant challenge to world's Li resources.*
- Can we replace Li by other cheaper, more abundant elements?
- Na is obvious choice: Na-analogues exist, esp. Na_xCoO_2

Na_xCoO_2



- Tunable number of Na^+ ions
- $x = 0$ to 1 per CoO_2

Na1 if C position 

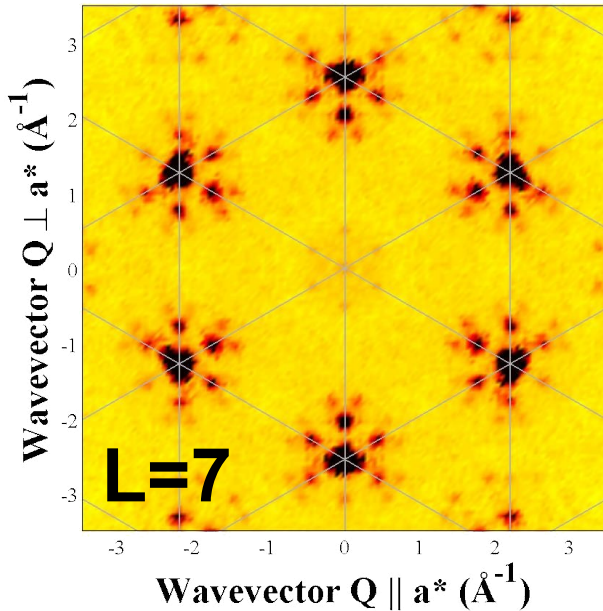
Na2 otherwise 

Superstructures

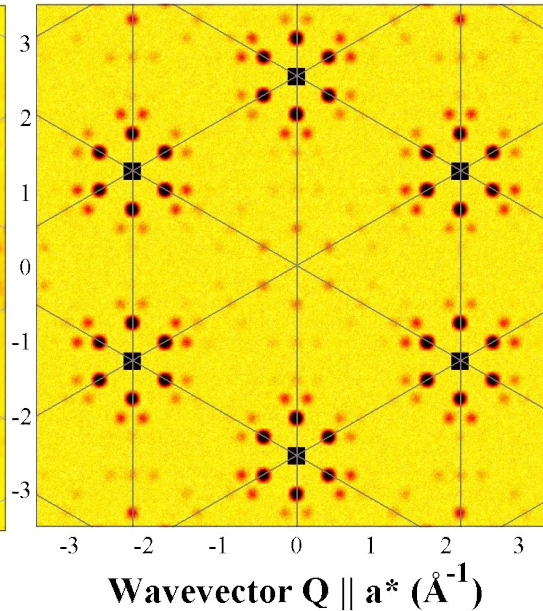
$T = 250 \text{ K}$

Ordered Stripe Phase

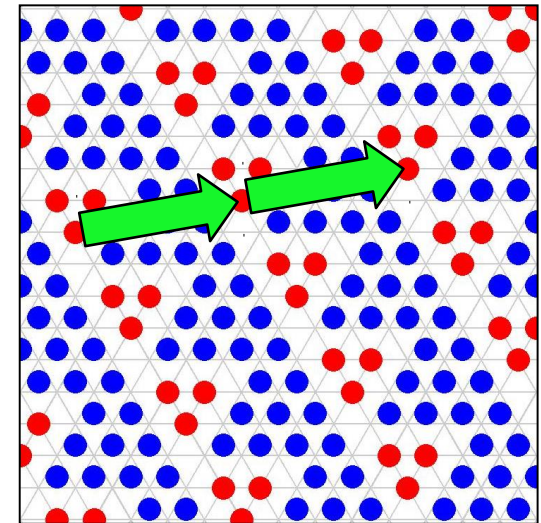
Experiment



Calculation



Model

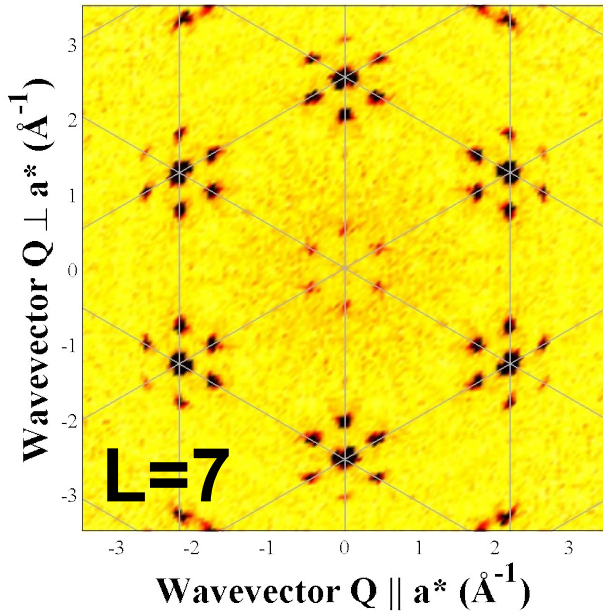


Unable to detect superlattice reflections using powder diffraction...
Need the sensitivity of single-crystal diffraction

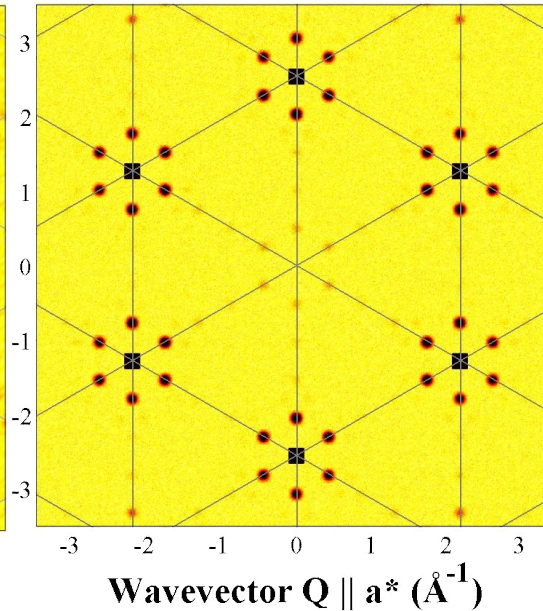
Superstructures

T = 350 K Disordered Stripe Phase

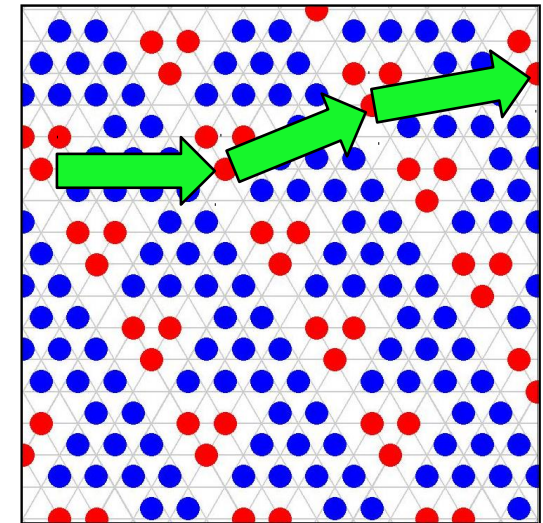
Experiment



Calculation



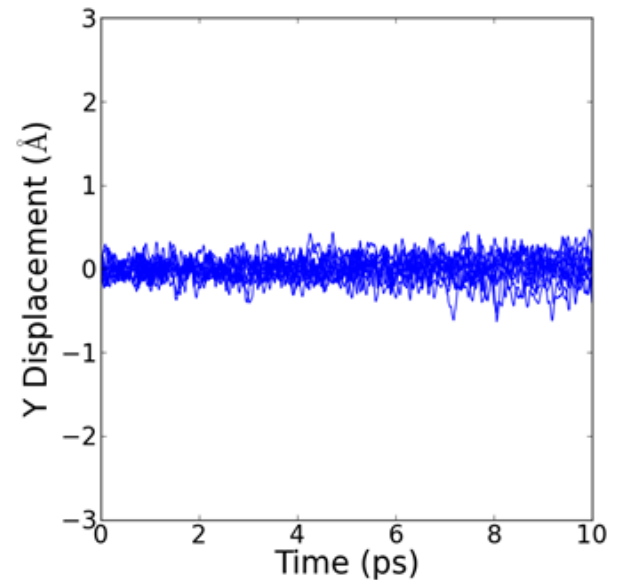
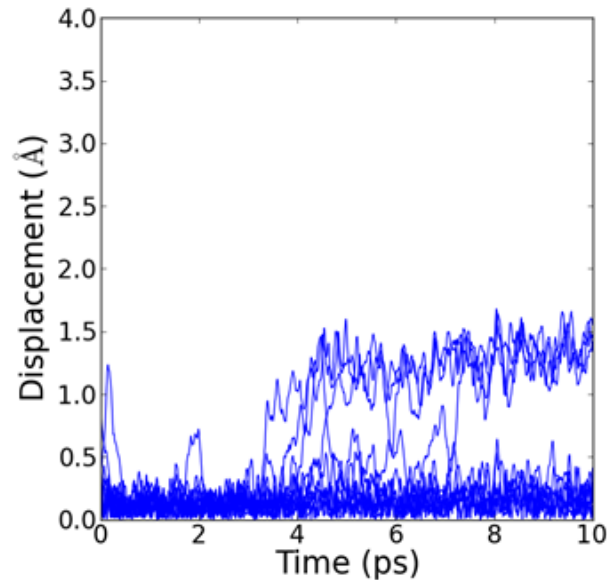
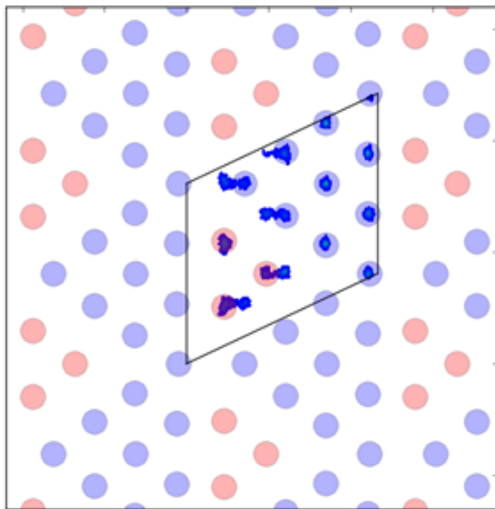
Model



Dynamic or static disorder along the stripes?

AIMD Simulations of diffusion

Ordered stripe phase ($T = 350$ K)



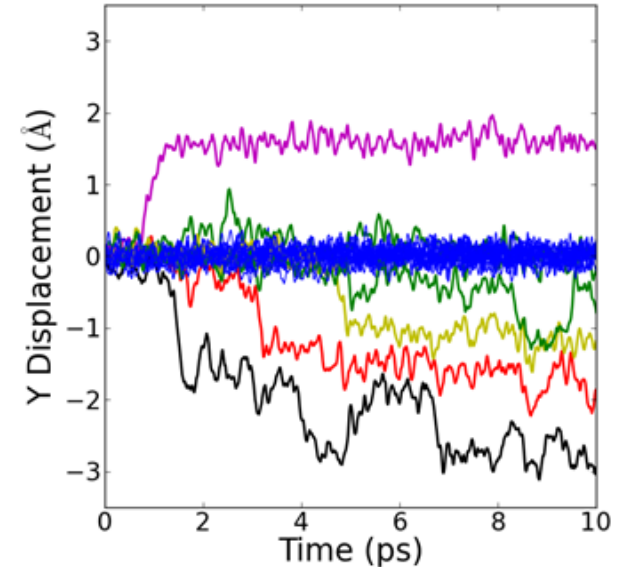
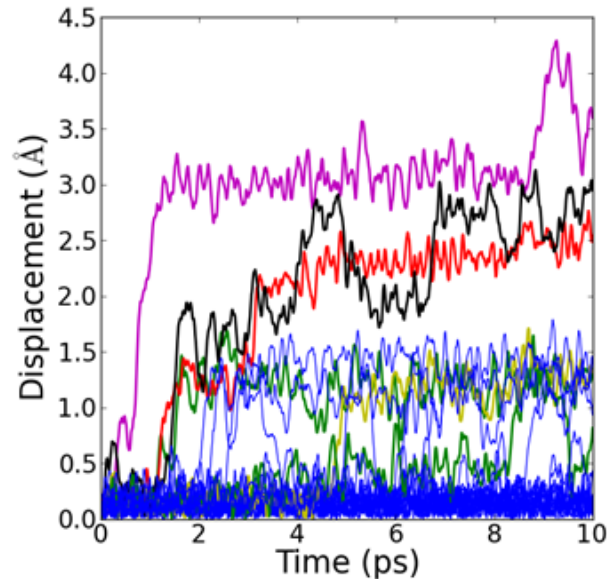
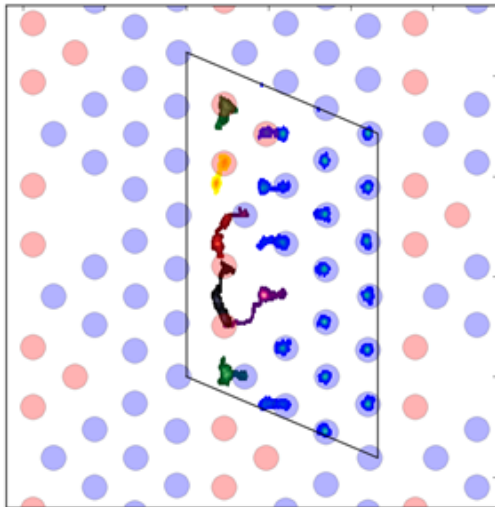
Ideal superstructure

- Na1 – Na2 hops perpendicular to stripes
- Translation of tri-vacancy clusters along stripes
- No bulk self-diffusion

T. J. Willis *et al.* Sci. Rep 8 3210 (2018)

AIMD Simulations of diffusion

Disordered stripe phase ($T = 350$ K)



Vacancy on Na1 site in stripe

- Na1 – Na2 hops with components along stripes
- Chains of correlated hops of different ions
- Bulk self-diffusion along stripes

Acknowledgements

- Collaborators

Jon Goff, David Voneshen, Dan Porter, Toby Willis:
RHUL

Bill David, Philippe Aeberhard, Oxford

Matthias Gutmann, ISIS

- FUNDING – EPSRC, STFC
- Computer time EPSRC, STFC

